IRF4/BATF and interleukin-33 orchestrate development and maintenance of adipose tissue resident regulatory T cells

Ajithkumar Vasanthakumar[1,2], Kazuyo Moro[6,7,8], Annie Xin[1,2], Yang Liao[1,2], Renee Gloury[1,2], Shimpei Kawamoto[9], Sidonia Fagarasan[9], Lisa A. Mielke[1,2], Shoukat Afshar-Sterle[1,2], Seth L. Masters[1,2], Susumu Nakae[7,10], Hirohisa Saito[11], John M. Wentworth[1,2], Peng Li[12], Wei Liao[12], Warren J. Leonard[12], Gordon K. Smyth[1,4], Wei Shi[1,3], Stephen L. Nutt[1,2], Shigeo Koyasu[5,6], Axel Kallies[1,2]

[1] The Walter and Eliza Hall Institute of Medical Research, 1G Royal Parade, Parkville, Victoria, 3050, Australia.

[2] The Department of Medical Biology, University of Melbourne, Parkville, Victoria, 3010, Australia

[3] Department of Computing and Information Systems, University of Melbourne, Parkville, Victoria, 3010, Australia.

[4] The Department of Mathematics and Statistics, University of Melbourne, Parkville, Victoria, 3010, Australia.

[5] Department of Microbiology and Immunology, Keio University Graduate School of Medicine, 35 Shinanomachi, Tokyo 160-8582, Japan.

[6] Laboratory for Immune Cell System, RIKEN Research Center for Integrative Medical Sciences, 1-7-22 Suehiro-cho, Yokohama 230-0045, Japan.

[7] Precursory Research for Embryonic Science and Technology (PRESTO), Japan Science and Technology Agency, 7 Goban-cho, Chiyoda-ku 102-0076, Japan.

[8] Division of Immunobiology, Department of Medical Life Science, Graduate School of Medical Life Science, Yokohama City University, 1-7-29 Suehiro-cho, Yokohama 230-0045, Japan.

[9] Laboratory for Mucosal Immunity, RIKEN Research Center for Integrative Medical Sciences, 1-7-22 Suehiro-cho, Yokohama 230-0045, Japan.

[10] Laboratory of Systems Biology, Center for Experimental Medicine and Systems Biology, The Institute of Medical Science, The University of Tokyo, Tokyo 108-8639, Japan.

[11] Department of Allergy and Immunology, National Research Institute for Child Health and Development, Tokyo 157-8535, Japan

[12] Laboratory of Molecular Immunology and Immunology Center, National Heart, Lung, and Blood Institute, National Institutes of Health, Bethesda, MD 20892-1674, USA.

Thymus-derived Foxp3$^+$ regulatory T cells (Tregs) undergo further differentiation in the periphery that promotes their migration into non-lymphoid tissues where they maintain immune homeostasis. Visceral adipose tissue (VAT) Tregs are functionally specialized tissue-resident cells that prevent obesity-associated inflammation and preserve insulin sensitivity and glucose tolerance. VAT-Treg development depends on the transcription factor PPARγ; however, the environmental cues required for their maintenance and for sustaining their transcriptional signature are unknown. Here we found that interleukin (IL)-33 signaling through ST2 and Myd88 was essential for development and maintenance of VAT-Tregs. Furthermore, the transcriptional regulators BATF and IRF4 were necessary for VAT-Treg differentiation through directly regulating ST2 and PPARγ expression. IL-33 administration induced vigorous population expansion of VAT-Tregs in normal mice as well as in genetically obese and high fat diet fed mice that are characterized by reduced VAT-Treg numbers. Expansion of Tregs tightly correlated with decrease in adipose tissue inflammation and improved metabolic parameters. Human adipose tissue Tregs also showed high ST2 expression, suggesting an evolutionarily conserved requirement for IL-33 in VAT-Treg homeostasis.

Foxp3$^+$ regulatory T cells (Tregs) are critically important for maintaining immune homeostasis and preventing lethal immune pathology. Treg differentiation and function are controlled by the transcription factor Foxp3, and Treg deficiencies in mouse or human result in severe systemic autoimmune pathology. This phenotype is recapitulated by the induced ablation of either Foxp3 or Tregs in adult mice, indicating a life-long requirement for Tregs[1,2]. Although some Tregs can develop from conventional CD4$^+$ T cell precursors in the periphery, the majority of Tregs develops in the thymus. Once they have entered the periphery, thymus-derived Tregs can further differentiate and undergo functional specialization endowing them with the ability to suppress polarized immune responses and inflammation in non-lymphoid tissues[3-8]. Thus, Tregs are a heterogeneous population that shows a high degree of phenotypic and functional specialization. We and

others have discovered that Tregs undergo stimulus-specific differentiation that is regulated by distinct transcription factors, including IRF4, T-bet, STAT3, RORγt, GATA3 and BCL6 (reviewed in [5-7]). For example T-bet is expressed in Tregs under Th1 inflammatory conditions and is required for their function in this particular environment[9]. Similarly, Bcl6 is induced in Tregs within the germinal centre and is essential for the development of a specialized population of follicular Tregs[10]. In keeping with these findings, specialized tissue-resident Treg populations were described recently. Similar to Tregs that develop under polarized inflammatory conditions, Tregs resident in non-lymphoid sites require tissue specific factors that promote their development and function[6]. Visceral adipose tissue (VAT)-resident Tregs constitute one of the better-known specialized populations of Tregs that are critically involved in preserving insulin sensitivity and glucose tolerance[11-13]. VAT-Tregs express the transcription factor Peroxisome proliferator-activated receptor gamma (PPARγ), which regulates cellular metabolism in the adipose tissue and is required for their development. The critical importance of Treg diversification in the periphery is evidenced by the severity of phenotypes observed in mice with Treg-specific ablation of transcription factors or chemokine receptors required for their functional specialization (reviewed in [4-7]).

As outlined above, several of the transcription factors essential for the development of specialized Treg populations have been identified; however, the cytokine signals that guide differentiation, population expansion and maintenance of specialized tissue-resident Tregs have remained largely unknown. While interleukin (IL)-2 is required for the development of a functional Tregs compartment and tightly regulates its size[14,15], recent results suggest that cytokines other than IL-2 may be involved in regulating the homeostasis of Treg with an effector phenotype[16]. Indeed, inflammatory cytokines were shown to contribute to the development and maintenance of specialized Treg populations. In particular, IL-27 and IFNγ induce expression of T-bet in Tregs[9,17] thereby promoting the suppression of Th1 polarized immune responses. Other pro-inflammatory cytokines, including IL-6, IL-12, and Type 1 interferons, however, impair regulatory function. Thus, maintenance of a diverse pool of peripheral Treg cells is a dynamically regulated process and the role of cytokines and inflammation is complex (reviewed in [18]).

We have previously identified a subset of Tregs that express the transcription factor Blimp1 and secret the immunosuppressive cytokine IL-10 (ref. [19]). Blimp1-expressing Tregs have an activated phenotype, display low amounts of L-selectin (CD62L) and CCR7 and are referred to as effector Tregs (eTregs)[5]. In contrast, Blimp1-negative Tregs express the chemokine receptor CCR7, primarily reside in lymphoid tissues and have been termed central Tregs (cTregs)[8,16]. eTregs represent a minor population in the lymphoid organs, but dominate in non-lymphoid tissues such as the lung and gastrointestinal tract. Transfer experiments suggested that Blimp1-negative Tregs can differentiate into Blimp1-expressing Tregs is response to TCR-stimulation and cytokine signaling[19]. In conjunction with our functional data, these results suggest that Blimp1-positive eTregs constitute the active effector stage of the Treg lineage.

To understand the differentiation of eTregs in more detail and to uncover molecules required for their development, we have performed transcriptional profiling of cTregs and eTregs. One of the genes specifically upregulated in eTregs was *Il1rl1*, encoding the IL-33 receptor (ST2). While eTregs residing in the lymphoid organs expressed low amounts of ST2, we found that VAT-Tregs from mouse and humans had markedly up-regulated ST2. IL-33 was both necessary and sufficient to drive VAT-Treg proliferation in wild-type mice and was able to rescue VAT-Treg numbers in genetically obese mice and mice fed a high fat diet (HFD), which correlated with improved metabolic parameters. The transcriptional regulators BATF and IRF4 were essential for the expression of *Il1rl1* and *Pparg* and were thus indispensable for VAT-Treg development. Together these data demonstrate a critical role for IL-33 in maintaining VAT-Tregs homeostasis.

Results

Effector Tregs express genes involved in active suppression and functional specialization

In order to uncover molecular pathways that facilitate the differentiation of eTregs, we performed high-resolution gene expression analysis by RNA-sequencing (RNAseq) of central and effector Treg populations sorted from spleens and lymph nodes

of *Blimp1*^{GFP} reporter mice. Consistent with the notion that eTregs differentiate from thymic derived cTreg precursors, they expressed Neuropilin 1 similar to or higher than their cTreg counterparts[20] (Fig. 1a). Despite comparable expression of *Foxp3*, more than 2,700 transcripts were differentially expressed between eTregs and cTregs, many of which have been shown to be important for Treg biology. Notably, transcripts encoding molecules important for Treg function, including IL-10, CTLA4, the cytotoxic molecule granzyme B, the co-inhibitory molecule Tigit and the ectonucleotidase CD39 were distinctly up-regulated in eTregs in comparison to cTreg, supporting the idea that eTregs constitute a highly suppressive population of Tregs (Fig. 1b,c, Suppl. Fig. 1 and Suppl. Table 1). Furthermore, we found elevated levels of transcripts encoding transcription factors such as T-bet, GATA3, and RORγt, suggesting that eTregs had undergone peripheral diversification and functional specialization. In line with this, eTregs showed altered expression of transcripts encoding molecules associated with T cell activation and terminal differentiation such as LAG-3, PD-1 and KLRG1. Finally, we found altered expression of genes encoding chemokine receptors and adhesion molecules, including down-regulation of *Ccr7* and *Sell* (encoding CD62L) and up-regulation of *Cxcr3*, *Ccr6*, *Ccr4* and *Ccr2*. Importantly, multiple genes found to be differentially expressed between both Treg populations were confirmed on the protein level (Fig. 1d,e and Suppl. Table 2). Consistent with this expression pattern, eTregs within lymphoid organs were preferentially localized outside of the T cell zone (Fig. 1f-g). Thus, Blimp1^{+} eTregs display a distinct transcriptional profile consistent with functional differentiation and active suppression, and localize outside of the T cell zone of lymphoid organs.

eTregs in particular in the visceral adipose tissue express the IL-33 receptor ST2

Tregs depend on IL-2 for their survival and homeostasis. As IL-2 is predominantly produced by T cells, our observation that eTregs primarily localized to areas outside of the T cell zone raised the possibility that an alternative mechanism may support eTreg survival. We therefore sought to identify cytokine receptors preferentially expressed by eTregs. Unexpectedly, *Il1rl1*, encoding the receptor for IL-33 (ST2), was the most differentially expressed cytokine receptor in our analysis and was up-regulated in eTregs (Fig. 2a,b). IL-33 has been associated with the differentiation and function of

various lymphocytes including type 2 helper T (Th2) cells, type 2 innate lymphoid cell (ILC2), and cytotoxic T cells[21-25]; however, its role in Treg biology is unknown. Flow-cytometric analysis confirmed ST2 expression on a fraction of eTregs; however, the majority of Tregs in spleen, lymph nodes, the lamina propria of the small intestine or the lung did not express ST2. In contrast, Tregs residing in the VAT were almost uniformly high for ST2 (Fig. 2c,d) and its expression tightly correlated with that of known VAT-Treg markers such as KLRG1, CCR2, Ly6C, and CD69 (ref. [13]) as well as PD-1 and Tigit (Suppl. Fig. 2). Confirming the notion that VAT-Tregs adhere to the eTreg definition, most VAT-Tregs were Blimp1$^+$ and expressed IL-10, which tightly correlated with ST2 expression (Fig. 2e,f).

ST2 and IL-33 deficient mice have severely reduced numbers of VAT-Tregs

To test if ST2 was required for the development of VAT-Tregs, we examined Treg populations in ST2-deficient (*Il1rl1*$^{-/-}$) mice. These mice showed no gross alterations in lymph node and splenic Treg populations. Furthermore, the presence of CD103$^+$ and KLRG1$^+$ Tregs indicated that ST2 was not generally required for the development of eTregs, which was supported by the comparable prevalence of Tregs in the small intestine and lungs of ST2-deficient and wild-type mice (Suppl. Fig. 3a-c). However, examination of VAT-resident lymphocytes revealed a striking reduction in proportion and number of Tregs (Fig. 3a,b). The requirement for ST2 expression was Treg intrinsic as mixed bone marrow chimeras, generated using congenically marked Ly5.1 wild-type and ST2-deficient hematopoietic cells, showed a similar reduction in the proportion of ST2-deficient Tregs (Fig. 3c). Consistent with these results, IL-33 deficient mice showed a dramatic reduction of Tregs in the VAT but not in other tissues analyzed (Fig. 3d, Suppl. Fig. 3e). The reduction of Tregs in the VAT was not a secondary effect of obesity as the *Il1rl1*$^{-/-}$ and *IL33*$^{-/-}$ mice had VAT amounts comparable to their littermate controls and showed similar body weight at the time of analysis (Suppl. Fig. 3e). As shown previously on a BALB/c background[26] and in agreement with a role for VAT Tregs in controlling metabolic parameters, ST2-deficient mice on a C57/B6 background showed impaired glucose tolerance even on a normal diet (Suppl. Fig. 3f). Similar results were obtained from *IL33*$^{-/-}$ mice, which showed impaired glucose

tolerance and increased insulin resistance (Suppl. Fig. 3g,h). CD11b+CD11c+ VAT macrophages were increased in the absence of IL-33 whereas inflammatory monocytes and CD8 T cells were unchanged (Suppl. Fig. 3i). Leptin levels in *IL33*$^{-/-}$ mice and their wild-type counterparts were similar, ruling out the possibility of VAT Treg reduction a consequence of leptin deficiency (Suppl. Fig. 3j). In summary our data demonstrate a non-redundant role of IL-33 in the development of Tregs in adipose tissue.

IL-33 induces proliferation and population expansion of VAT-Tregs *in vitro* and *in vivo*

To directly examine how IL-33 signaling impacted on ST2^{+} Tregs, we isolated Tregs from the VAT, labeled them with the cell division tracker CTV and cultured them in the presence of IL-33 or IL-2. Both IL-2 and IL-33 induced vigorous proliferation of Foxp3^{+} VAT-Tregs even in the absence of T cell receptor (TCR) stimulation (Fig. 4a). Strikingly, however, IL-33 induced proliferation was more pronounced than proliferation induced by IL-2, and was not dependent on the production of IL-2 by other cells as it occurred even in the presence of IL-2 blocking antibodies (Suppl. Fig. 4a,b).

IL-33 is tightly regulated by posttranslational processing and has been shown previously to be expressed in adipose tissue[26,27]. In agreement with this notion, we found full length and processed IL-33 protein expressed by total VAT indicating that VAT-Tregs have *in situ* access to IL-33. Amounts of IL-33 protein but not transcripts increased with age, as did expression of ST2 on the surface of VAT-Tregs, which correlated with an increase in their numbers (Suppl. Figs. 4c-f). To examine the effects of IL-33 signaling *in vivo*, we injected IL-33 or vehicle (PBS) intra-peritoneally into 8-week-old wild-type mice that have relatively few VAT-Tregs. In parallel, we injected mice of the same group with IL-2/anti-IL-2 monoclonal antibody complexes (IL-2c), which selectively expand Tregs[28]. Similar to previous published results, IL-33 administration resulted in a marginal increase of Tregs in the spleen[29] but not in small intestine and lung. In line with our observation that ST2 and KLRG1 were co-expressed on eTregs, population expansion of Tregs in the spleen after IL-33 injection was restricted to the KLRG1^{+} fraction of eTregs. In contrast, IL-2c expanded Treg populations systemically (Suppl. Fig. 4g-i). Strikingly, Treg numbers in the VAT after IL-33 administration were

increased at least 10 fold, while the extent of VAT-Treg population expansion upon IL-2c administration was significantly lower (Fig. 4b). The expanded Treg population in the VAT was maintained at a high level for at least 8 days after IL-33 administration before it contracted (Suppl. Fig. 4j).

VAT-Tregs depend on the transcription factor PPARγ[13]. Consistent with this notion, we detected high amounts of *Pparg* transcripts in VAT-Tregs. Importantly, IL-33 maintained *Pparg* in proliferating VAT-Tregs. While this was similar to the activity of IL-2, IL-33 induced proliferation resulted in increased expression of Foxp3 and Gata3, indicating that IL-33 supported the maintenance of the Treg transcriptional signature (Fig. 4c). Collectively, these data demonstrate that VAT-Tregs are exclusively equipped to respond to IL-33, which promotes their proliferation and maintains the Treg transcriptional signature.

IL-33 signaling in Tregs requires Myd88

IL-33 has been shown to signal through the adaptor protein Myd88 (ref. [30]); however, the role of Myd88 in Treg development, maintenance or function has not been studied in detail. Examination of Myd88-deficient (*Myd88*$^{-/-}$) mice showed similar proportions or only a modest reduction of Tregs in the lymph nodes and spleen, small intestine or lungs. Furthermore, *Myd88*$^{-/-}$ mice had similar proportions of KLRG1^{+} Tregs, indicating that Myd88 is not required for Treg development or eTreg differentiation. *Myd88*$^{-/-}$ mice, however, lacked most Tregs in the adipose tissue (Fig. 4d,e, Suppl. Fig. 5a-c). This was not secondary to increased obesity as both wild-type and mutant mice showed similar body weight and VAT mass at the time of analysis (Suppl. Fig. 5d). The requirement for Myd88 was Treg intrinsic as mixed bone marrow chimeric mice containing congenically marked wild-type and Myd88-deficient hematopoietic cells showed a similar reduction of *Myd88*$^{-/-}$ Tregs specifically in the adipose tissue (Fig. 4f).

TCR-signaling induces the VAT-Treg transcriptional program

To test which signals could promote VAT-Treg development and maintenance, we activated splenic Tregs in the presence of anti-CD3 and CD28 and various cytokines. Activation via TCR crosslinking and co-stimulation in the presence of IL-2 induced

vigorous proliferation and expression of ST2 on a fraction of Tregs. The presence of IL-33 resulted in increased ST2 expression; however, incubation with other proinflammtory cytokines such as IL-12, IL-6 and IL-4 did not (Fig. 5a and Suppl. Fig. 5e). This was dependent on Myd88, as Myd88-deficient Tregs, when cultured in the presence of IL-2 and IL-33, failed to express ST2 despite vigorous proliferation (Fig. 5b, Suppl. Fig. 5f). TCR signaling also resulted in pronounced upregulation of *Pparg* transcripts, but consistent with our earlier results IL-33 did not induce further upregulation (Fig. 5c). In line with a requirement for TCR signals for the development and maintenance of Tregs in the adipose tissue, examination of VAT-Tregs in comparison to splenic Tregs showed increased expression of Nur77 and low expression of TCF7, two transcription factors that are up or down-regulated in response to TCR signaling, respectively (Fig. 5d).

Overall these data indicate that TCR crosslinking induces PPARγ and ST2 expression, while IL-33 signaling results in further upregulation of ST2 expression and population expansion of VAT-Tregs.

Batf and IRF4 are required for PPARγ and ST2 expression and for the development of VAT-Tregs

The AP-1 transcriptional regulator BATF is required for many aspects of T and B cell function[31]. BATF/JUN complexes promote DNA binding of the transcription factor IRF4, and both factors cooperate during Th17 development and $CD8^+$ T cell effector differentiation[32-36]. BATF expression is induced by TCR signals and its activity has been implicated in the gene expression program down-stream of IL-33 (ref. [37]). To test potential roles for BATF and IRF4 in the development of VAT-Tregs we examined mice deficient in either of these factors. *Batf*-deficient mice had mildly reduced proportions of Tregs in the spleen, but strikingly, Tregs in the VAT were almost completely ablated. Similarly, analysis of *Irf4*$^{-/-}$ mice revealed near absence of Tregs from the VAT, while the numbers of Tregs in the spleen were only moderately affected (Fig. 5e,f, Suppl. Fig. 6 a,b). Notably, body weight and VAT mass was similar in mutant mice and their wild-type counterparts (Suppl. Fig. 6c,d). The requirement for BATF and IRF4 was Treg intrinsic as analysis of chimeric mice containing wild-type and mutant Tregs revealed a severe

reduction of BATF and IRF4-deficient Tregs in the VAT in comparison to wild-type cells (Suppl. Fig. 6e). Remaining Tregs in the VAT of *Batf*$^{-/-}$ and *Irf4*$^{-/-}$ mice did not express ST2, and cultured splenic Tregs from either of these mice, despite vigorous proliferation, failed to up-regulate ST2 (Fig. 5g, Suppl. Fig. 6f-h). Similarly, IRF4-deficient Tregs stimulated *in vitro* were unable to induce *Pparg* transcripts (Fig. 5h). Thus, both BATF and IRF4 were required for the induction of key components of the transcriptional program that guides VAT-Treg development.

To test if IRF4 and BATF could directly regulate *Pparg* and *Il1rl1* expression, we interrogated our chromatin immunoprecipitation (ChIP) sequencing data based on activated CD4$^+$ T cells[34]. This revealed binding of IRF4 and BATF to intronic regions in both genes, which contained AP-1-IRF4 composite elements (AICE)[32,34]. ChIP experiments confirmed that IRF4 also bound to these regions in primary Tregs (Fig. 6a-d).

Mice with a Treg-specific deletion of *Irf4* develop severe autoimmunity and succumb to disease between 6 and 8 weeks of age precluding VAT-Treg analysis (ref. [38] and our own observations). To test if the expression of IRF4 was required not only for the development of VAT-Tregs but also for their maintenance, we crossed transgenic mice expressing Cre-recombinase under the control of granzyme B gene (*GzmB*) regulatory elements to mice carrying a conditional *Irf4* allele. *GzmB* expression within the Treg lineage is restricted to eTregs (Suppl. Fig. 6i), therefore, leading to deletion of *Irf4* only after eTreg differentiation. While the proportion of Tregs in the spleen was largely unchanged in floxed *Irf4*xGzmBCre$^+$ mice, there was marked reduction of Tregs in the VAT, and the remaining VAT-Tregs had lost ST2 and KLRG1 expression (Fig. 6e,f). Body weight and VAT mass, however, were similar in both groups (Suppl. Fig. 6j).

In summary, VAT-Tregs require BATF and IRF4 for the induction of the VAT-Treg differentiation program, and continuous expression of IRF4 is essential for its maintenance.

IL-33 administration can rescue VAT-Tregs in genetically obese and HFD fed mice

VAT-Tregs can reduce obesity-associated inflammation and insulin resistance, and genetically obese mice, such as mice deficient in leptin or its receptor, display

severely reduced numbers of VAT-resident Tregs[11,13]. To test a putative link between obesity-mediated loss of VAT-Tregs and IL-33 signaling, we examined the VAT of New Zealand Obese (NZO) mice, which exhibit early onset of obesity and hyperglycemia[39]. While splenic Tregs were mildly reduced, VAT-Treg numbers were strongly impaired in NZO mice compared to age and sex matched C57BL/6 mice (Fig. 7a). Furthermore, VAT-Tregs isolated from NZO mice expressed reduced amounts of KLRG1 and ST2 that are usually associated with VAT-Tregs (Fig. 7b). Strikingly, IL-33 administration led to a dramatic increase in Treg numbers in the VAT of NZO mice and induced expression of ST2 and KLRG1 usually associated with the VAT-Treg phenotype (Fig. 7c, Suppl. Fig. 7a). Notably, this was associated with a decrease in fasting glucose concentrations close to levels observed in C57/B6 mice and improved glucose tolerance (Fig. 7d, Suppl. Fig. 7b).

We next wanted to test the activity of IL-33 in a more physiological context such as HFD induced obesity. Similar to previous reports[11,13], we observed a reduction in VAT-Tregs in HFD mice, despite an increase of full-length and processed IL-33 protein expression (Fig. 7e,f), suggesting that other factors contribute to the diet-induced loss of VAT-Tregs. IL-33 administration could rectify Treg numbers, which correlated with improved glucose tolerance both in NZO mice and mice on a HFD (Fig. 7g, Suppl. Fig. 7b,c). In addition, we observed decreases in VAT macrophages as well as proinflammatory monocytes and $CD8^+$ T cells upon IL-33 treatment in both mouse models (Fig. 7h, Suppl. Figs 7d,e). IL-33 administration resulted in decreases in Mcp1, RANTES, Mip1α and IL1β expression at the transcript level in the VAT of NZO and HFD mice, which, however, in most cases did not reach significance in the period of treatment, and it did not result in altered leptin serum levels (Suppl. Figs 7f,g). We also observed modest reduction in the VAT mass, and decrease in the adipocyte size in mice treated with IL-33 compared to their PBS treated controls (Suppl. Fig. 8a,b). Notably, IL-33 did not improve insulin sensitivity in either of these mouse strains as measured by Akt phosphorylation after insulin administration (Suppl. Fig. 8d).

IL-33 is expressed by human adipocytes and stromal cells[40,41], implying that the adipose tissue itself creates a niche for the resident Treg population to regulate glucose and insulin homeostasis. In agreement with this notion, we found that Tregs resident in

human adipose tissue expressed ST2, whereas Treg cells in peripheral blood did not (Suppl. Fig. 8e). ST2 expression in human VAT Tregs suggests that the requirement for development and maintenance of adipose tissue Tregs for IL-33 is evolutionarily conserved.

Discussion

Tregs in the VAT constitute a relatively well-characterized population of tissue resident cells. They are critical in preserving metabolic homeostasis by suppressing inflammation in the adipose tissue, thereby limiting the development of obesity induced insulin resistance[13,42]. In this study, we have shown that the IL-33 receptor ST2 was expressed at high levels on VAT-Tregs. Mice lacking either IL-33 or ST2 showed a specific and near complete absence of Tregs in the adipose tissue. Administration of IL-33 specifically expanded Tregs in the adipose tissue not only in wild-type mice but also in genetically obese mice, which are characterized by hyperglycemia and drastically reduced VAT-Treg numbers, indicating a critical role for IL-33 in maintaining Tregs during obesity.

IL-33 is a cytokine of the IL-1 family that is particularly noted for its critical involvement in respiratory allergy and asthma[43,44]. It has been shown to promote the development and function of multiple cell types, most prominently Th2 cells, ILC2 and effector $CD8^+$ T cells[21-25]. IL-33 is produced by a range of different cell types, including endothelial and myeloid cells and is released upon tissue damage[27]. It has therefore been termed an 'alarmin' that signals inflammation and tissue damage to responsive cell populations. The excess VAT associated with obesity constitutes a constitutively inflammatory environment characterized by infiltration and activation of immune cells that overproduce cytokines and chemokines (reviewed in [45]). Along with inflammation, obesity is also paralleled by an increase in IL-33 production, and expression of ST2 during high-fat diet induced obesity and diabetes was found to be protective[26,40,41]. However, the cellular and molecular bases for these observations were unknown. We propose that the beneficial effects of IL-33 are mediated through promotion of Treg expansion in the adipose tissue. We have shown that this is paralleled by a pronounced reduction of proinflammatory

VAT-macrophages and monocytes and reduced numbers of $CD8^+$ T cells, thus leading to an adipose tissue milieu that promotes glucose tolerance. Notably, Il-33 administration to obese mice did not result in reduced insulin levels and insulin signaling in the VAT as measured by Akt phosphorylation. Thus, it is conceivable that IL-33 by an unknown mechanism may directly impact on insulin secretion. Obesity has been shown to result in a loss of VAT-Tregs. As this occurs despite an increase in IL-33 protein expression, it is likely that VAT-Treg homeostasis is impacted upon by factors that act in addition to IL-33 during obesity development. IL-33-mediated VAT-Treg population expansion may counterbalance low-grade inflammation until the point when IL-33 signalling becomes limiting, resulting in a loss of Tregs as well as increased tissue inflammation and insulin resistance. Similar to IL-1, IL-33 is released during inflammation and processed post-translationally by caspases, which alters its biological activity[27]. It is thus conceivable that active levels of IL-33 change depending on the integrity and cytokine environment of a particular tissue. Obesity alters the cellular composition and inflammatory parameters of adipose tissue and we show here this results in increased protein expression and altered processing of IL-33. Thus, it will be interesting to examine the levels of biologically active and available IL-33 in obese individuals.

In this study we have identified essential components of the transcriptional circuit regulating ST2 expression and IL-33 signaling. We have found that the transcriptional regulators IRF4 and BATF cooperate on the *Il1rl1* gene locus to induce the expression of ST2. In the absence of either factor ST2 expression was not detectable on Tregs and VAT-Treg development was abolished. Interestingly, both IRF4 (as a target of the NfkB pathway) and BATF are downstream of IL-33 signaling, suggesting that IL-33 may promote the expression of its own receptor by maintaining high levels of IRF4 and BATF. In support of such a model, we found that Myd88, an essential component of the IL-33 signaling pathway, was required for the upregulation of ST2 expression on splenic Tregs. Importantly, IL-33 not only promoted proliferation of VAT-Tregs but also increased their expression of Foxp3 and Gata3. While maintaining Foxp3 is critical for preventing the conversion of Tregs to autoreactive and inflammatory T cells[46,47], Gata3 is necessary for Treg function[48,49]. Gata3 is also essential for ST2 expression by Th2 cells, while IL-33 itself promotes Gata3 expression and enhances IL-2 mediated Stat5

phosphorylation in these cells[50]. Thus, our data suggest that a similar regulatory circuit is active in Tregs and that IL-33 together with IL-2 is critical for preserving the identity and regulatory function of eTreg in the adipose tissue. Notably, IL-33 is the first cytokine identified that is essential for a specific population of tissue resident Tregs. This indicates that Tregs not only depend on IL-2 but require other cytokines that promote population expansion and maintenance of cellular identity in a tissue specific manner.

We have previously identified eTregs as a distinct subpopulation of Tregs that develop from thymic Foxp3$^+$ Tregs in response to TCR signals and inflammatory cytokines[19]. Analysis of transcriptional profiling data of eTregs and their cTreg counterparts revealed that eTregs showed increased levels of multiple transcription factors, including T-bet, RORγt and GATA3 that are implicated in functional specialization of diverse conventional and regulatory T cell populations. This suggests that Tregs in healthy steady state conditions can continuously initiate differentiation into various subtypes of eTregs. These cells may be recruited or expanded depending on the environmental stimulus and their anatomical localization. This model is supported by our observation that *Pparg*, encoding PPARγ, the transcription factor specifically required for the development of VAT-Tregs, is upregulated in eTregs isolated from lymphoid organs, raising the possibility that cTregs give rise to the immediate precursors of VAT-resident Tregs. Such a model is also reinforced by our finding that TCR-signals were sufficient to induce *Pparg* transcription in cTregs *in vitro* and by the observation that VAT-Tregs tightly adhered to the eTreg definition, ie displaying an effector phenotype and expressing high levels of Blimp1 and IL-10. However, it remains to be tested whether such a linear differentiation pathway from lymphoid cTregs to specialized eTregs resident in non-lymphoid tissue indeed exists or whether the 'fate' of a particular Treg is determined by TCR specificity or other signals earlier during thymic selection. Interestingly, our data show that IRF4, which tightly integrates TCR and cytokine signaling, population expansion and effector differentiation in conventional T cells[35,51] is also critical for the TCR mediated up-regulation of *Pparg* and ST2 suggesting that IRF4 in Tregs, similar to Th17 cells[33], is at the center of a regulator network that links environmental signals with differentiation outcomes.

Over the last few years the functional diversification and specialization of Tregs has emerged as a critical factor in maintaining immune homeostasis in non-lymphoid tissues. Given the deleterious effects of generalized Treg deletion or the immune suppressive impact of increasing Treg numbers on pathogen-specific immune responses or tumor clearance, targeting Tregs in a tissue-specific manner is of great clinical interest. Both genetic and high fat diet induced obesity is strongly correlated to reduction in VAT Tregs numbers. Mathis and colleagues have elegantly demonstrated that increase in VAT inflammation, expansion of inflammatory cells and glucose intolerance as consequence of VAT Treg reduction[13]. Based on the results presented here, the IL-33/ST2 axis emerges as a novel pathway that may allow therapeutic expansion of Tregs in adipose tissue to prevent inflammation, insulin resistance and impaired glucose tolerance during obesity and type 2 diabetes development. Importantly, we show that similar to the mouse model, Tregs isolated from human adipose tissue expressed high levels of ST2, suggesting an evolutionarily conserved requirement for IL-33 in Treg homeostasis in the VAT. This suggests that other tissue-specific pathways may exist that can be harnessed to target distinct Treg populations without affecting the majority of Tregs resident in lymphoid organs or other tissues.

Experimental Procedures

Human ethics This project was approved by the Walter and Eliza Hall Human Research Ethics Committee. Human blood and omental adipose tissue from obese participants were collected into EDTA tubes and DME medium respectively, and processed within three hours.

Mouse models. *IL33*$^{-/-}$ mice[52], *Myd88*$^{-/-}$ mice[53], NZO mice[39] and transgenic mice expressing Cre-recombinase under the control of granzyme B gene (*GzmB*) regulatory elements[54] were described previously. *Batf*$^{-/-}$ mice[55], *Il10*^{GFP} mice[56] and *Foxp3*^{RFP} mice[57] were ordered from Jax, *Irf4*$^{-/-}$ mice[58] were from Tak Mak and *Irf4*$^{fl/fl}$ mice[59] from Ulf Klein. ST2-deficient mice (*Il1rl1*$^{-/-}$)[60] were kindly provided by Dr. Kenji Nakanishi of

Hyogo College of Medicine. All mouse lines have been maintained on a C57BL/6J (Ly5.2) background except *IL33*$^{-/-}$, which is on a C57BL/6N background. For some of the experiments they were crossed to *GzmB*Cre[54] or *Blimp1*^{GFP} (ref. [61]) mice. Mixed bone marrow chimeras were generated from lethally irradiated (2 x 550R) wild-type Ly5.1 mice reconstituted with a mixture of mutant or control bone marrow (Ly5.2) and Ly5.1 bone marrow as indicated and mice were allowed 6-8 weeks to reconstitute. Mice were maintained and used in accordance with the guidelines of the Walter and Eliza Hall Institute Animal Ethics Committee and RIKEN animal care and use committee. If not specified otherwise, all mice used for VAT analysis or metabolic testing in this study were 35-39 weeks old males.

IL-33 and IL-2/anti-IL-2 complex injections. 0.5 μg of recombinant murine IL-33 in PBS (R&D systems) was intraperitoneally injected to mice 4 times (day 0, 2, 4 and 6) and analyzed on day 8 post injection. IL-2/anti-IL-2 complexes were made by mixing 1.5 μg recombinant mouse IL-2 (eBioscience) with 7.5 μg monoclonal antibody to mouse IL-2 (JES6.1; produced 'in house') and incubating for 30 min at 37°C. Mice were injected intraperitoneally on day 0, 1 and 2 with either IL-2/anti-IL-2 complexes or PBS as a control and were analyzed on day 7.

Human tissue. Omental fat was collected from patients undergoing weight loss surgery with their consent and transported to laboratory on ice. The tissue was processed as described below for mouse adipose tissue. From the same human subjects 3 ml peripheral blood was also collected.

Preparation of lymphocytes from the fat. Unless indicated otherwise, epididymal fat was collected from 30-35 week old male mice, finely minced and suspended in 0.025% collagenase Type IV (Gibco) (2ml collagenase per gram fat). The suspension was incubated for 45 min at 37°C in a shaker. After incubation the suspension was 10 times diluted with PBS + 2% FCS and spun at 800 g for 15 min at 4°C. The upper adipocyte fraction was discarded and the stromal vascular fraction that has settled down was further purified to obtain lymphocytes by Histopaque (Sigma) gradient.

Isolation of intestinal lamina propria lymphocytes (LPL). Intestinal LPLs were extracted from the small intestine. In brief, Peyer's patches removed and intestines were opened longitudinally and cut into small pieces (<5 mm). Epithelial cells and intraepithelial lymphocytes (IEL) were removed by washing with hanks balanced salt solution and incubating with 5 mM EDTA for 30 min at 37°C. The intestinal pieces were washed with RPMI 10% FCS, and LPLs were isolated by digestion with 1 μg/ml DNase (Sigma-Aldrich) and 200 μg/ml Collagenase III (Worthington) for 40 min at 37°C. The LPL fractions were purified by 40/80% Percoll (GE Healthcare) gradient.

Antibodies and flow cytometry. Fluorochrome-conjugated antibodies directed against the following mouse antigens were used for analysis by flow cytometry: CD4 (RM 4-5), CD62L (MEL-14), Ly5.2 (104), CD44 (IM7), Ly-6C (AL-21), CD11b (M1/70) from BD Pharmingen; CCR2 from R&D Biosystems; TCF1 (c6309) from Cell Signalling; ICOS (7E-17G9), Foxp3 (FJK-16s), PD-1 (J43), CD103 (2E7), KLRG1 (2F1), CD25 (PC61.5), Tigit (GIGD7), TCRb (H57-597), CXCR3 (CXCR3-173), Ly5.1 (A20), ST2 (RMST2-2), Ly6C (HK1.4), GATA3 (TWAJ), CD11c (N418), F4/80 (BM8), CD19, CD8 from eBioscience. Fluorochrome-conjugated antibodies directed against the following human antigens were used for analysis by flow cytometry: hCD25 (M-A251), hCD4 (RPA T4) from BD Pharmingen, hST2/IL-1R4 from R&D Biosystems, hFoxp3 (206D) from Biolegend, hCD45RA (HI 100) from eBioscience. Surface staining was done at 4°C for 30 mins. Antibody stained cells were analysed using BD FACS Canto II or BD Fortessa1.

Intracellular staining. Intracellular staining was performed using eBioscience Foxp3 staining kit as per the manufacturer's protocol.

Cell Trace Violet labeling. CTV labeling was done as described by the manufacturers (Molecular Probes). Briefly, 1 μl of 5 mM Cell Trace Violet was added to 10 $x10^6$ in 1ml of PBS and incubated at 37°C for 10 min with intermittent shaking. The reaction was quenched with 10 ml of ice-cold RPMI medium.

Enrichment of Tregs and cell culture. Home made anti-CD8 and anti-B220 (rat IgG) were used to deplete $CD8^+$ T cells and B cells from spleen and lymph node. Briefly, these depleting antibodies were incubated with RBC lysed splenocytes for 30 min at 4°C. Unbound antibody was washed and the antibody-coupled cells were incubated with BioMag Goat Anti-Rat IgG beads (Qiagen) to deplete $CD8^+$ T cells and B cells. Anti-CD25-biotin antibody (7D4, eBioscience) was used to positively select Tregs from the CD8 and B cells depleted splenocytes. T cells were cultured using plate bound anti-CD3 (10 μg/ml, 145-2C11), soluble anti-CD28 (2 μg/ml, 37.51) antibodies and 100 U/ml IL-2 (R&D systems) as previously described[62].

Glucose tolerance tests. 1.5 g/kg (or 1 g/kg for NZO mice) (body mass) glucose was injected intraperitoneally to mice fasted for 8 h. Blood samples were obtained from the tail tip at the indicated times, and blood glucose levels were measured using hand held glucometer (Accu-Chek performa, Roche).

Western blotting. Fat tissue was homogenized in lysis buffer (HEPES, EGTA, b-glycerophosphate, DTT, Na3VO4, glycerol, TritonX, protease inhibitor (Roche), phosphatase inhibitor (Sigma Aldrich), NaF and PMSF), and protein concentration was determined using the Bradford method. 20μg protein was loaded and resolved on 4-12% gradient polyacrylamide gels (NuPAGE, life technologies), transferred to nitrocellulose membranes (Bio-Rad), and blocked for 1h with 5% milk. Immunoblotting was performed using the primary antibodies as specified. The following antibodies were used: anti-pAkt (S473) (clone D9E, Cell Signaling), anti-Akt1 (c-20, Santa Cruz), and anti-mIL-33 (R&D Systems).

RNA extraction and real time quantitative PCR. Total RNA was isolated from epididymal fat with Qiazol reagent (Qiagen) and reverse transcribed to cDNA with the use of random hexamers. Real-time PCR was performed using SYBER Green kit with the primers for the genes specified, using the following primers: *Pparg*-F: 5'-TCACAAGAGCTGACCCAATG-3'; *Pparg*-R: 5'-TGAGGCCTGTTGTAGAGCTG-3';

Il33-F: 5'-GGTGTGGATGGGAAGAAGCTG-3'; *Il33*-R: 5'-GAGGACTTTTTGTGAAGGACG-3'; *GAPDH*-F: 5'-ACGGCCGCATCTTCTTGTGCA-3'; *GAPDH*-R: 5'-AATGGCAGCCCTGGTGACCA-3'; *Mip1a*-F: 5'-GGAATTCACCATGAAGGTCTCCACCACTG-3'; *Mip1a*-R: 5'-GCGGATCCAAGACTCTCAGGCATTC-3'; *RANTES*-F: 5'-GGAATTCGGGTACCATGAAGATCTC-3'; *RANTES*-R: 5'-GCGGATCCTAGCTCATCTCCAAATA-3'; *Mcp1*-F: 5'-GGAATTCACCACCATGCAGGTCCCTGTC-3'; *Mcp1*-R: 5'-GCGGATCCGAGTCACACTAGTTCACT-3'; *Il1b*-F: 5'-CTGCAGCTGGAGAGTGTGGAT-3'; *Il1b*-R: 5'-GGGAACTCTGCAGACTCAAACT-3'

Histology. Formaldehyde fixed epididymal fat was stained using Hematoxylin and eosin and the slides were scanned using Aperio (Leica). Adipocyte numbers and size were calculated using Fiji (imageJ).

High fat diet. Male C57BL/6 mice were fed with high calorie food (36% fat, Specialty feeds, SF03-002) for 40 weeks.

Insulin and Leptin measurements, and HOMA-IR calculation. Serum from mice was collected and multiplex ELISA was performed using Milliplex MAP mouse metabolic magnetic bead panel (Millipore) as per the manufacturer's instructions. HOMA-IR was calculated from the fasting blood insulin and glucose values using the program downloaded from Diabetes trials unit, University of Oxford (https://www.dtu.ox.ac.uk/homacalculator/).

Chromatin Immunoprecipitation (ChIP). ChIP was performed following an adapted protocol by Upstate/Millipore (Massachusetts, USA). In brief, Tregs isolated from spleens and lymph nodes were stimulated *in vitro* with anti-CD3 (5 µg/ml), anti-CD28 (1.8 µg/ml) and recombinant hIL-2 (100 U/ml) for 72 h. Live cells were isolated by Histopaque gradient centrifugation. Cross-linking was done by addition of 1%

paraformaldehyde at room temperature for 10 min, followed by sonication and immunoprecipitation with 10 μg of anti-IRF4 (clone sc-6059) and a corresponding goat polyclonal-IgG control (clone sc-2028) (Santa Cruz Technologies). Primers used in ChIP experiments were as follows: *Il1rl1*-F: 5'-CTGTGGAGCGAGATCATACG-3'; *Il1rl1*-R: 5'-GCCAAGACTTGAGCTGATGA-3'; *Pparg*-ChIP-F: 5'-TCATGCACTTGGTATGACAGG-3'; *Pparg*-ChIP-R: 5'-TCTCCATTACCCCATCCTTG-3'.

Immunofluorescence staining. For immunohistochemical analysis, mesenteric lymph nodes (MLNs) from C57BL/6 mice were fixed and stained as previously described[63]. Before Foxp3 and Blimp1 staining, formaldehyde-fixed sections were treated with HistoVT One (Nacalai Tesque) at 70ºC for 20 min for antigen retrieval. The following primary antibodies were used for immunohistochemistry: anti-CD3ε (500-A2, Beckton Dickinson), anti-B220 (RA3-6B2, eBioscience), anti-Foxp3 (FJK-16s, eBioscience), anti-Blimp1 (6D3, eBioscience). The stained slides were examined with a Zeiss Axioplan 2 fluorescence microscope. To evaluate the location of $Blimp1^{+}Foxp3^{+}$ or $Blimp1^{-}Foxp3^{+}$ cells in MLNs, we randomly took pictures of microscopic fields that included B cell follicles and T cell zones in several MLNs and checked the location of these cells manually using these pictures. The frequency of these cells in each location (T cell zone, B cell follicle, T-B boarder, and inter-follicular zone) is shown in pie chart.

RNA-sequencing and bioinformatic analysis. Lymphocytes were isolated from spleens and lymph nodes of *Blimp1*^{GFP} mice and enriched for Tregs using magnetic beads coupled to an anti-CD25 antibody. Tregs were sorted to purity of typically >97% using TCRb, CD4, CD25 and CD62L antibodies. RNA purification was performed following the manufacturer's protocol using the RNAeasy Plus Mini Kit (Qiagen). RNA samples were sequenced on an Illumina Genome Analyzer, producing more than 35million 36bp single-end reads per sample. Reads were mapped to mouse genome *mm9* using *Subread*[64], with the minimum number of consensus reads set to two. Mapped reads were assigned to mouse RefSeq genes using *featureCounts*[64] and NCBI mouse annotation build 37.2. Read counts were analyzed using Bioconductor software[65]. Genes were

filtered as not expressed if they had a total read count less than five. Differential expression analysis was performed using generalized linear models functions of the *edgeR* package[66], with the negative binomial dispersion set to a common value of 0.02. A false discovery rate cut-off of 0.05 was applied. Heatmaps were generated using the gplots package in with negative log2 RPKM values reset to zero. A gene had to have a RPKM value of 8 or greater in at least one of the two conditions and show an expression change of at least 2 fold to be called differentially expressed.

Statistics. If not stated otherwise an unpaired student t test was performed to test for statistical significance; error bars denote mean ± S.D. unless specified otherwise.

Author contribution. A.V. planned and performed most experiments; K.M. performed experiments related to the IL-33 and ST2-deficient mice; A.X., S.A.-S., Y.L., P.L., W.L., W.S., W.J.L. and G.K.S. did or analyzed the RNA and ChIP sequencing experiments; S.K. and S.F. did the immunofluorescence; L.M. and R.G. performed additional experiments; S.N. and H.S. contributed key reagents; S.L.M. and J.M.W. contributed to the scientific planning and organization of experiments; S.L.N. and S.K. designed experiments; A.K. oversaw and designed the study and together with A.V. wrote the manuscript.

Acknowledgments. We thank Paul O'Brien (Royal Melbourne Hospital) for assistance with tissue collection and Mark Febbraio (Baker IDI) and Andrew Lew (The Walter and Eliza Hall Institute) for critical advice. We are grateful to Kenji Nakanishi, Tak Mak, Ulf Klein, Susan Kaech for mice. This work was supported by grants and fellowships from the National Health and Medical Research Council of Australia (AK, SLN, GKS), the Sylvia and Charles Viertel Foundation (AK), the Australian Research Council (AK, SLN), the Diabetes Australia Research Trust (JMW), PRESTO from the Japan Science and Technology Agency (KM), a Grant-in Aid for Young Scientist (A) (22689013) (KM), a Grant-in-Aid for Scientific Research (S) (22229004) (SK), a Grant-in-Aid for Scientific Research (C) (21590971) (KM) from the Japan Society for the Promotion of Science (JSPS), and a Grant-in-Aid for Scientific Research on Innovative Areas

(23118526) (KM) from the Ministry of Education, Culture, Sports, Science and Technology, Japan. WL, PL, and WJL were supported by the Division of Intramural Research, National Heart, Blood, and Lung Institute, NIH, Bethesda, MD, USA. This study was made possible through Victorian State Government Operational Infrastructure Support and Australian Government NHMRC Independent Research Institute Infrastructure Support scheme.

Figure legends

Figure 1. Blimp1^{+} eTregs have a distinct transcriptional profile and localize outside of the T cell area. (**a**) Flow cytometric analyses of splenic Tregs from *Foxp3*^{RFP}*Blimp1*^{GFP} mice showing the proportion of Blimp1^{+} Tregs and Neuropilin (Nrp1) expression. (**b**). Scatter plot showing a comparison of normalized RNA-sequencing (RNAseq) reads from Blimp1^{-} cTregs and Blimp1^{+} eTregs. Selected transcripts indicated show significantly higher (below the diagonal line) or lower (above the diagonal line) expression in eTregs. (**c**) Expression of genes related to Treg function as determined by RNAseq. (**d**) Heat maps showing expression of transcriptional regulators (left) and genes related to migration and adhesion (right) that are differentially expressed between cTregs and eTregs. (**e**) Flow cytometric analysis of Foxp3^{+} cells from the peripheral lymph nodes (LNs) of *Foxp3*^{RFP}*Blimp1*^{GFP} mice, assessed for Blimp1-expression along with surface molecules encoded by genes differentially expressed between cTregs and eTregs. Flow cytometric data are representative of 3-5 experiments. (**f**) Immunofluorescence staining of mesenteric LN sections from C57BL/6 mice. Upper panel shows high-magnification of section showing cells labeled with anti-Foxp3 and anti-Blimp1 antibodies. Lower panels show low-magnification sections with CD3 (green) demarcating the T cell zone and B220 (red) representing B cells. DAPI (blue) indicates nuclear staining. Arrows indicate Foxp3/Blimp1 double-positive cells. (**g**) Quantification of cTreg and eTreg localization. The frequency of Tregs in each location (T cell zone, B cell follicle, T-B boarder, and inter-follicular zone) is shown in pie charts.

Figure 2. The IL-33 receptor ST2 is specifically expressed by eTregs, in particular in the VAT. (**a**) Expression levels of transcripts encoding cytokine receptors extracted from RNAseq analysis. (**b**) RNAseq track showing read mapping to the *Il1rl1* gene in cTregs and eTregs. (**c**) Expression of ST2 on cTregs and eTregs. (**d**) ST2 expression on Tregs from spleen and visceral adipose tissue (VAT) of a *Foxp3*^{RFP}*Blimp1*^{GFP} mouse (left). Bar graph (right) showing percentages of Tregs expressing ST2 in organs as indicated. Values are means ± S.D. from at least five mice. LPL - Small intestine lamina propria lymphocytes. (**e-f**) Flow cytometric analyses of *Foxp3*^{RFP}*Blimp1*^{GFP} **(e)** or *Foxp3*^{RFP}*Il10*^{GFP} (f) mice showing CD4^{+} T cells from spleen (left) and VAT (right). Flow cytometric data are representative of 3-5 experiments.

Figure 3. The IL-33 receptor ST2 is required for the differentiation of VAT-Tregs. (**a**) Flow cytometric analysis of CD4^{+} T cells in the spleen and VAT of wild-type (WT) and ST2-deficient (*Il1rl1*$^{-/-}$) mice. (**b**) Quantification of Treg in the VAT of WT and *Il1rl1*$^{-/-}$ mice. (**c**) Flow cytometric analysis of Tregs in the VAT of mixed bone marrow chimeric mice containing wild-type (Ly5.1) and ST2-deficient (Ly5.2, *Il1rl1*$^{-/-}$) hematopoietic cells. (**d**) Proportions and numbers of Treg in the VAT of WT and *Il33*$^{-/-}$ mice. Flow cytometric data in (a), (c) and (d) are representative of five to seven 35-week-old male mice analyzed per group.

Figure 4. IL-33 induces proliferation and maintains identity of VAT-Treg. (**a**) Equal numbers of purified wild-type (WT) VAT lymphocytes were labeled with the cell division tracker Cell Trace Violet (CTV) and cultured for 3.5 days in the presence of IL-2 or IL-33 as indicated. Data are representative of three experiments. Numbers in dot plots are percentages of Foxp3^{+} cells. Graph (right) shows mean fold increase of Tregs at the end of the culture. (**b**) *In vivo* expansion of VAT-Tregs upon IL-33 administration. Flow cytometric analysis of VAT CD4^{+} T cells from 8-week-old male WT mice assessed for Foxp3 and ST2 expression (left) and numbers of Tregs (right) after administration of vehicle (PBS) or IL-33 as indicated. Symbols in graphs indicate data points for individual mice and horizontal lines indicate means ± S.D. One-way ANOVA, $P<0.0001$. (**c**)

Expression of *Pparg* transcripts (left) in VAT-Tregs cultured as indicated in comparison to splenic Tregs, and expression of Foxp3 and GATA3 protein (right) in cultured VAT-Tregs. (**d**) Flow cytometric analysis of $CD4^+$ T cells in the spleen and the VAT of wild-type (WT) mice and *Myd88*$^{-/-}$. (**e**) Quantification of Tregs in the VAT of WT and *Myd88*$^{-/-}$ mice. (**f**) Representative flow cytometric plots (left) and bar graph (right) showing percentages of WT and Myd88-deficient $Foxp3^+$ cells in the VAT of mixed bone marrow chimera containing WT (Ly5.1) and *Myd88*$^{-/-}$ (Ly5.2) hematopoietic cells. Values are mean ± S.D. from 3 mice per group. Flow cytometric plots are representative of at least 3 different experiments or at least 5 mice per genotype. ** P<0.007; *** P=0.0002.

Figure 5. TCR signals induce the VAT-Treg transcriptional program in a BATF and IRF4 dependent manner. (a) Expression of ST2 on Tregs enriched from spleens of wild-type (WT) and cultured in conditions as indicated for 3 days. (**b**) Expression of ST2 on Tregs from WT or *Myd88*$^{-/-}$ mice cultured as in (A) in the presence of IL-2 and IL-33. (**c**) Expression of *Pparg* transcripts in splenic Tregs freshly isolated or cultured as indicated. (**d**) Flow cytometric analysis of $CD4^+$ T cells and Tregs isolated from the spleen (left) or VAT. (**e-f**) Flow cytometric analysis of $CD4^+$ T cells (e) and numbers (f) of Tregs in the VAT from WT, *Irf4*$^{-/-}$ and *Batf*$^{-/-}$ mice. (**g**) Expression of ST2 on Tregs enriched from spleens of the indicated genotypes and cultured in conditions as in (a) including IL-33. (**h**) Expression of *Pparg* transcripts in splenic Tregs freshly isolated from WT or IRF4-deficient mice or cultured as indicated. Flow cytometry plots are representative of 3-5 individual experiments. Plots in panels a, b and g derive from an experiment with all genotypes represented. One-way ANOVA was performed for (f) and (h), P<0.0001. P value for panel (c) *** P=0.0001.

Figure 6. IRF4 and BATF bind to the *Pparg* and *Il1rl1* gene loci, and continuous IRF4 expression is required for maintaining VAT-Treg identity. (**a-b**) ChIP sequencing analyses for IRF4 and BATF on activated $CD4^+$ T cells showing read mapping and binding motif analyses for the *Pparg* (A) and *Il1rl1* (B) gene loci. (**c-d**) ChIP analyses performed using purified activated splenic Tregs and an IRF4-specific antibody or an IgG control. qPCR analysis of the immuno-precipitated DNA was done

with primers specific for the intronic binding regions for IRF4 and AP1 identified in the *Pparg* (c) or *Il1rl1* (d) gene loci. (**e**) Flow cytometric analysis of $CD4^+$ T cells from spleens and VAT of $Irf4^{fl/fl}/GzmBCre^+$ (right) and control (left) mice. Graph shows absolute numbers of Tregs from the VAT. (**f**) Phenotype of VAT-Tregs from $Irf4^{fl/fl}/GzmBCre^+$ (blue) and control (red) mice. Symbols in graphs indicate data points for individual mice and horizontal lines indicate means ± S.D. *** P=0.0001.

Figure 7. IL-33 administration increases VAT-Treg numbers in genetically obese mice. (**a**) (**a**) Flow cytometric analysis of $CD4^+$ T cells from the spleen and VAT of C57BL/6 and genetically obese NZO mice and proportions of Tregs within $CD4^+$ T cells in spleens and VAT of mice as indicated. (**b**) Phenotype of VAT Tregs in C57BL/6 and NZO mice. (**c**) Numbers and phenotype of Tregs in the VAT of PBS and IL-33 treated NZO mice. Values are mean from 5 mice per group. (**d**) Fasting blood glucose in C57BL/6 and NZO mice treated with PBS or IL-33 as indicated. (**e**) Numbers of Tregs in the VAT of mice fed with normal or high fat diet (HFD), and HFD mice treated with IL-33. Values are mean from 4 or 5 mice per group. (**f**) IL-33 protein expression analyzed by Western Blot of adipose tissue from mice on a normal Chow diet or on a HFD as indicated. $Il33^{-/-}$ mice were used as specificity control. Loading was controlled by detection of an unspecific band with the anti-IL-33 antibody. (**g**) Glucose tolerance test for HFD mice treated with PBS or IL-33. **(h)** Proportion of VAT proinflammatory monocytes, CD8 T cells and macrophages in PBS or IL-33 treated HFD mice. Values in d, e, g, h are means from 4-5 mice per group. Two way ANOVA test (P<0.0001) was performed for (g) and error bars denote S.E.M.; symbols in other graphs indicate data points for individual mice and horizontal lines indicate means ± S.D. * P<0.03; ** P<0.008; *** P<0.0004.

References

1 Josefowicz, S. Z., Lu, L. F. & Rudensky, A. Y. Regulatory T cells: mechanisms of differentiation and function. *Annual review of immunology* **30**, 531-564 (2012).

2 Ohkura, N., Kitagawa, Y. & Sakaguchi, S. Development and maintenance of regulatory T cells. *Immunity* **38**, 414-423 (2013).
3 Feuerer, M., Hill, J. A., Mathis, D. & Benoist, C. Foxp3+ regulatory T cells: differentiation, specification, subphenotypes. *Nature immunology* **10**, 689-695 (2009).
4 Campbell, D. J. & Koch, M. A. Phenotypical and functional specialization of FOXP3(+) regulatory T cells. *Nature reviews. Immunology* **11**, 119-130 (2011).
5 Cretney, E., Kallies, A. & Nutt, S. L. Differentiation and function of Foxp3(+) effector regulatory T cells. *Trends in immunology* **34**, 74-80 (2013).
6 Burzyn, D., Benoist, C. & Mathis, D. Regulatory T cells in nonlymphoid tissues. *Nature immunology* **14**, 1007-1013 (2013).
7 Chaudhry, A. & Rudensky, A. Y. Control of inflammation by integration of environmental cues by regulatory T cells. *The Journal of clinical investigation* **123**, 939-944 (2013).
8 Liston, A. & Gray, D. H. Homeostatic control of regulatory T cell diversity. *Nature reviews. Immunology* (2014).
9 Koch, M. A. *et al.* The transcription factor T-bet controls regulatory T cell homeostasis and function during type 1 inflammation. *Nature immunology* **10**, 595-602 (2009).
10 Linterman, M. A. *et al.* Foxp3+ follicular regulatory T cells control the germinal center response. *Nature medicine* **17**, 975-982 (2011).
11 Feuerer, M. *et al.* Lean, but not obese, fat is enriched for a unique population of regulatory T cells that affect metabolic parameters. *Nature medicine* **15**, 930-939 (2009).
12 Feuerer, M. *et al.* Genomic definition of multiple ex vivo regulatory T cell subphenotypes. *Proceedings of the National Academy of Sciences of the United States of America* **107**, 5919-5924 (2010).
13 Cipolletta, D. *et al.* PPAR-gamma is a major driver of the accumulation and phenotype of adipose tissue Treg cells. *Nature* **486**, 549-553 (2012).
14 Fontenot, J. D., Rasmussen, J. P., Gavin, M. A. & Rudensky, A. Y. A function for interleukin 2 in Foxp3-expressing regulatory T cells. *Nature immunology* **6**, 1142-1151 (2005).
15 Pierson, W. *et al.* Antiapoptotic Mcl-1 is critical for the survival and niche-filling capacity of Foxp3(+) regulatory T cells. *Nature immunology* **14**, 959-965 (2013).
16 Smigiel, K. S. *et al.* CCR7 provides localized access to IL-2 and defines homeostatically distinct regulatory T cell subsets. *The Journal of experimental medicine* **211**, 121-136 (2014).
17 Hall, A. O. *et al.* The cytokines interleukin 27 and interferon-gamma promote distinct Treg cell populations required to limit infection-induced pathology. *Immunity* **37**, 511-523 (2012).
18 Konstantinou, G. N. *et al.* Assessment of airflow limitation, airway inflammation, and symptoms during virus-induced wheezing episodes in 4- to 6-year-old children. *The Journal of allergy and clinical immunology* **131**, 87-93 e81-85 (2013).

19 Cretney, E. *et al.* The transcription factors Blimp-1 and IRF4 jointly control the differentiation and function of effector regulatory T cells. *Nature immunology* **12**, 304-311 (2011).
20 Weiss, J. M. *et al.* Neuropilin 1 is expressed on thymus-derived natural regulatory T cells, but not mucosa-generated induced Foxp3+ T reg cells. *The Journal of experimental medicine* **209**, 1723-1742 (2012).
21 Schmitz, J. *et al.* IL-33, an interleukin-1-like cytokine that signals via the IL-1 receptor-related protein ST2 and induces T helper type 2-associated cytokines. *Immunity* **23**, 479-490 (2005).
22 Moro, K. *et al.* Innate production of T(H)2 cytokines by adipose tissue-associated c-Kit(+)Sca-1(+) lymphoid cells. *Nature* **463**, 540-544 (2010).
23 Molofsky, A. B. *et al.* Innate lymphoid type 2 cells sustain visceral adipose tissue eosinophils and alternatively activated macrophages. *The Journal of experimental medicine* **210**, 535-549 (2013).
24 Licona-Limon, P., Kim, L. K., Palm, N. W. & Flavell, R. A. TH2, allergy and group 2 innate lymphoid cells. *Nature immunology* **14**, 536-542 (2013).
25 Bonilla, W. V. *et al.* The alarmin interleukin-33 drives protective antiviral CD8(+) T cell responses. *Science* **335**, 984-989 (2012).
26 Miller, A. M. *et al.* Interleukin-33 induces protective effects in adipose tissue inflammation during obesity in mice. *Circulation research* **107**, 650-658 (2010).
27 Kakkar, R. & Lee, R. T. The IL-33/ST2 pathway: therapeutic target and novel biomarker. *Nature reviews. Drug discovery* **7**, 827-840 (2008).
28 Boyman, O., Kovar, M., Rubinstein, M. P., Surh, C. D. & Sprent, J. Selective stimulation of T cell subsets with antibody-cytokine immune complexes. *Science* **311**, 1924-1927 (2006).
29 Turnquist, H. R. *et al.* IL-33 expands suppressive CD11b+ Gr-1(int) and regulatory T cells, including ST2L+ Foxp3+ cells, and mediates regulatory T cell-dependent promotion of cardiac allograft survival. *Journal of immunology* **187**, 4598-4610 (2011).
30 Martin, M. U. Special aspects of interleukin-33 and the IL-33 receptor complex. *Seminars in immunology* **25**, 449-457 (2013).
31 Murphy, T. L., Tussiwand, R. & Murphy, K. M. Specificity through cooperation: BATF-IRF interactions control immune-regulatory networks. *Nature reviews. Immunology* **13**, 499-509 (2013).
32 Glasmacher, E. *et al.* A Genomic Regulatory Element That Directs Assembly and Function of Immune-Specific AP-1-IRF Complexes. *Science* **338**, 975-980 (2012).
33 Ciofani, M. *et al.* A validated regulatory network for Th17 cell specification. *Cell* **151**, 289-303 (2012).
34 Li, P. *et al.* BATF-JUN is critical for IRF4-mediated transcription in T cells. *Nature* **490**, 543-546 (2012).
35 Man, K. *et al.* The transcription factor IRF4 is essential for TCR affinity-mediated metabolic programming and clonal expansion of T cells. *Nature immunology* **14**, 1155-1165 (2013).
36 Grusdat, M. *et al.* IRF4 and BATF are critical for CD8 T-cell function following infection with LCMV. *Cell death and differentiation* (2014).

37 Brint, E. K. *et al.* Characterization of signaling pathways activated by the interleukin 1 (IL-1) receptor homologue T1/ST2. A role for Jun N-terminal kinase in IL-4 induction. *The Journal of biological chemistry* **277**, 49205-49211 (2002).
38 Zheng, Y. *et al.* Regulatory T-cell suppressor program co-opts transcription factor IRF4 to control T(H)2 responses. *Nature* **458**, 351-356 (2009).
39 Kluge, R., Scherneck, S., Schurmann, A. & Joost, H. G. Pathophysiology and genetics of obesity and diabetes in the New Zealand obese mouse: a model of the human metabolic syndrome. *Methods in molecular biology* **933**, 59-73 (2012).
40 Wood, I. S., Wang, B. & Trayhurn, P. IL-33, a recently identified interleukin-1 gene family member, is expressed in human adipocytes. *Biochemical and biophysical research communications* **384**, 105-109 (2009).
41 Zeyda, M. *et al.* Severe obesity increases adipose tissue expression of interleukin-33 and its receptor ST2, both predominantly detectable in endothelial cells of human adipose tissue. *International journal of obesity* **37**, 658-665 (2013).
42 Cipolletta, D. Adipose tissue-resident regulatory T cells: phenotypic specialization, functions and therapeutic potential. *Immunology* (2014).
43 Boraschi, D. & Tagliabue, A. The interleukin-1 receptor family. *Seminars in immunology* **25**, 394-407 (2013).
44 Makrinioti, H., Toussaint, M., Jackson, D. J., Walton, R. P. & Johnston, S. L. Role of interleukin 33 in respiratory allergy and asthma. *The lancet. Respiratory medicine* **2**, 226-237 (2014).
45 Han, J. M. & Levings, M. K. Immune regulation in obesity-associated adipose inflammation. *Journal of immunology* **191**, 527-532 (2013).
46 Williams, L. M. & Rudensky, A. Y. Maintenance of the Foxp3-dependent developmental program in mature regulatory T cells requires continued expression of Foxp3. *Nature immunology* **8**, 277-284 (2007).
47 Sakaguchi, S., Vignali, D. A., Rudensky, A. Y., Niec, R. E. & Waldmann, H. The plasticity and stability of regulatory T cells. *Nature reviews. Immunology* **13**, 461-467 (2013).
48 Wang, Y., Su, M. A. & Wan, Y. Y. An essential role of the transcription factor GATA-3 for the function of regulatory T cells. *Immunity* **35**, 337-348 (2011).
49 Wohlfert, E. A. *et al.* GATA3 controls Foxp3(+) regulatory T cell fate during inflammation in mice. *The Journal of clinical investigation* **121**, 4503-4515 (2011).
50 Guo, L. *et al.* IL-1 family members and STAT activators induce cytokine production by Th2, Th17, and Th1 cells. *Proceedings of the National Academy of Sciences of the United States of America* **106**, 13463-13468 (2009).
51 Kwon, H. *et al.* Analysis of interleukin-21-induced Prdm1 gene regulation reveals functional cooperation of STAT3 and IRF4 transcription factors. *Immunity* **31**, 941-952 (2009).
52 Oboki, K. *et al.* IL-33 is a crucial amplifier of innate rather than acquired immunity. *Proceedings of the National Academy of Sciences of the United States of America* **107**, 18581-18586, doi:10.1073/pnas.1003059107 (2010).
53 Adachi, O. *et al.* Targeted disruption of the MyD88 gene results in loss of IL-1- and IL-18-mediated function. *Immunity* **9**, 143-150 (1998).

54 Jacob, J. & Baltimore, D. Modelling T-cell memory by genetic marking of memory T cells in vivo. *Nature* **399**, 593-597, doi:10.1038/21208 (1999).
55 Schraml, B. U. *et al.* The AP-1 transcription factor Batf controls T(H)17 differentiation. *Nature* **460**, 405-409 (2009).
56 Kamanaka, M. *et al.* Expression of interleukin-10 in intestinal lymphocytes detected by an interleukin-10 reporter knockin tiger mouse. *Immunity* **25**, 941-952 (2006).
57 Wan, Y. Y. & Flavell, R. A. Identifying Foxp3-expressing suppressor T cells with a bicistronic reporter. *Proceedings of the National Academy of Sciences of the United States of America* **102**, 5126-5131 (2005).
58 Mittrucker, H. W. *et al.* Requirement for the transcription factor LSIRF/IRF4 for mature B and T lymphocyte function. *Science* **275**, 540-543 (1997).
59 Klein, U. *et al.* Transcription factor IRF4 controls plasma cell differentiation and class-switch recombination. *Nat. Immunol* **7**, 773-782 (2006).
60 Hoshino, K. *et al.* The absence of interleukin 1 receptor-related T1/ST2 does not affect T helper cell type 2 development and its effector function. *The Journal of experimental medicine* **190**, 1541-1548 (1999).
61 Kallies, A. *et al.* Plasma cell ontogeny defined by quantitative changes in blimp-1 expression. *The Journal of experimental medicine* **200**, 967-977 (2004).
62 Kallies, A. *et al.* Transcriptional repressor Blimp-1 is essential for T cell homeostasis and self-tolerance. *Nature immunology* **7**, 466-474 (2006).
63 Kawamoto, S. *et al.* The inhibitory receptor PD-1 regulates IgA selection and bacterial composition in the gut. *Science* **336**, 485-489, doi:10.1126/science.1217718 (2012).
64 Liao, Y., Smyth, G. K. & Shi, W. The Subread aligner: fast, accurate and scalable read mapping by seed-and-vote. *Nucleic acids research* **41**, e108 (2013).
65 Gentleman, R. C., Carey, V.J., Bates, D.M., Bolstad, B., Dettling, M., Dudoit, S., Ellis, B., Gautier, L., Ge, Y., Gentry, J., et al. Bioconductor: open software development for computational biology and bioinformatics. *Genome Biol.* **5** (2004).
66 Lee, H. Y. *et al.* Blockade of IL-33/ST2 ameliorates airway inflammation in a murine model of allergic asthma. *Experimental lung research* **40**, 66-76 (2014).

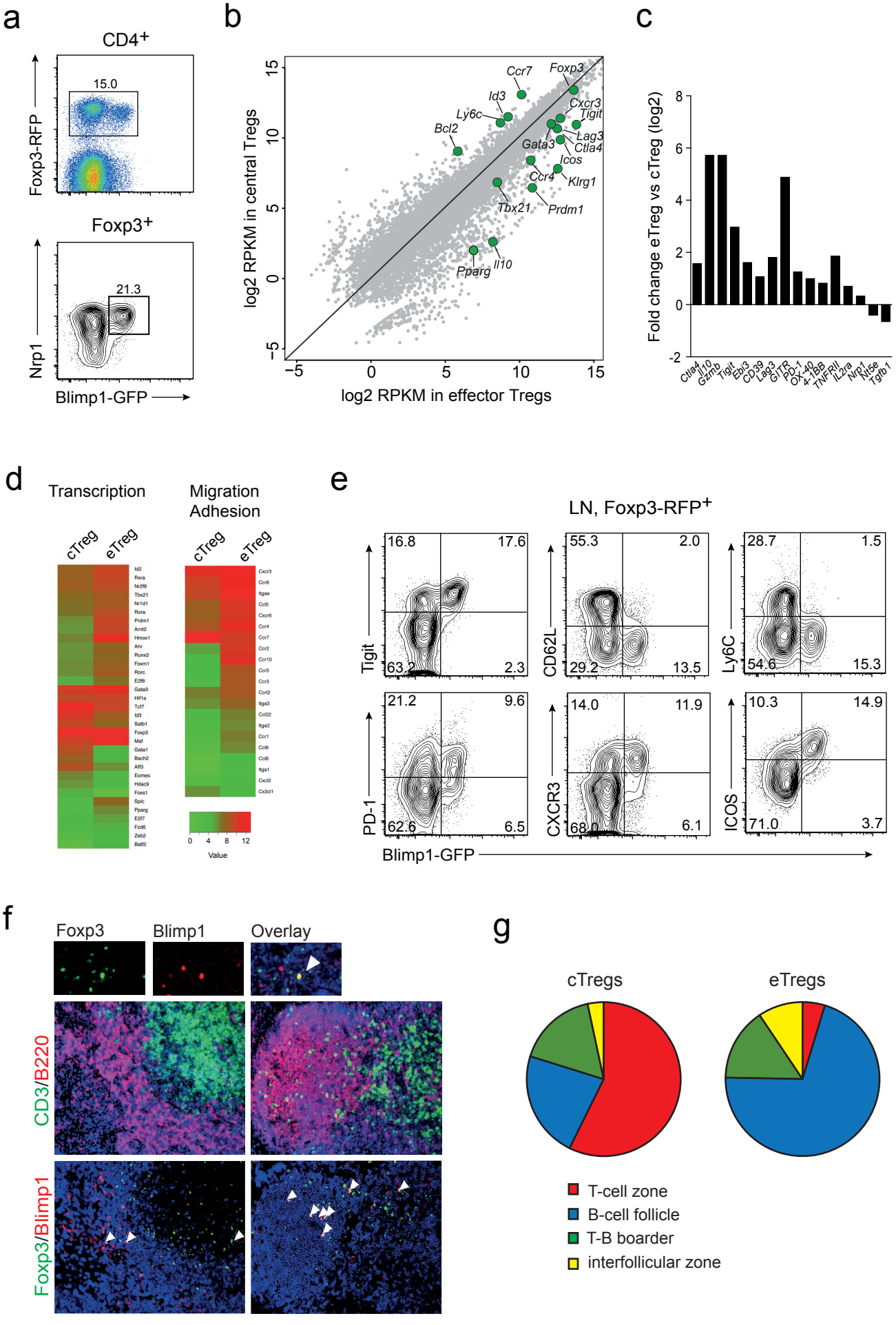

Vasanthakumar et al. Fig. 1

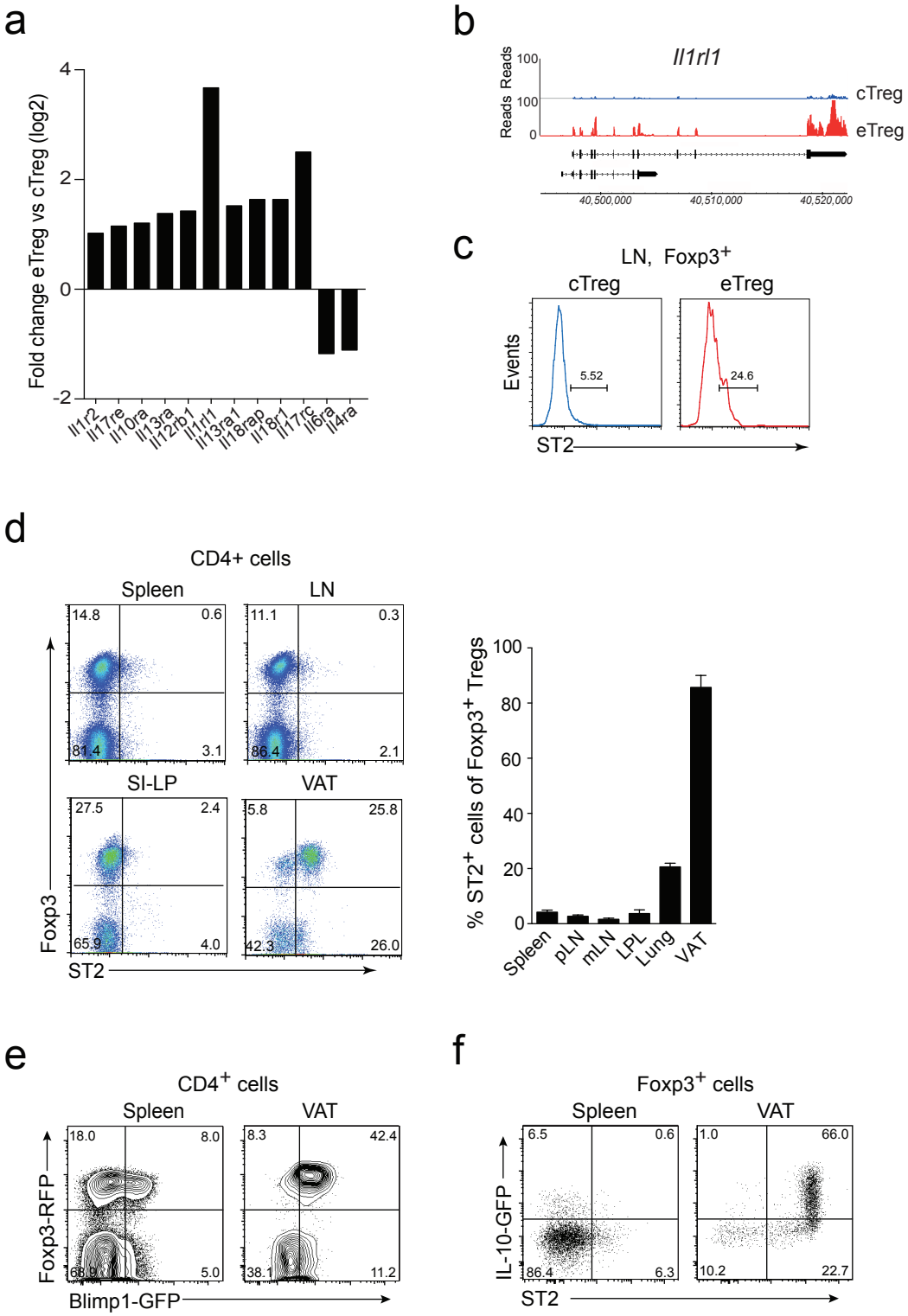

Vasanthakumar et al. Fig. 2

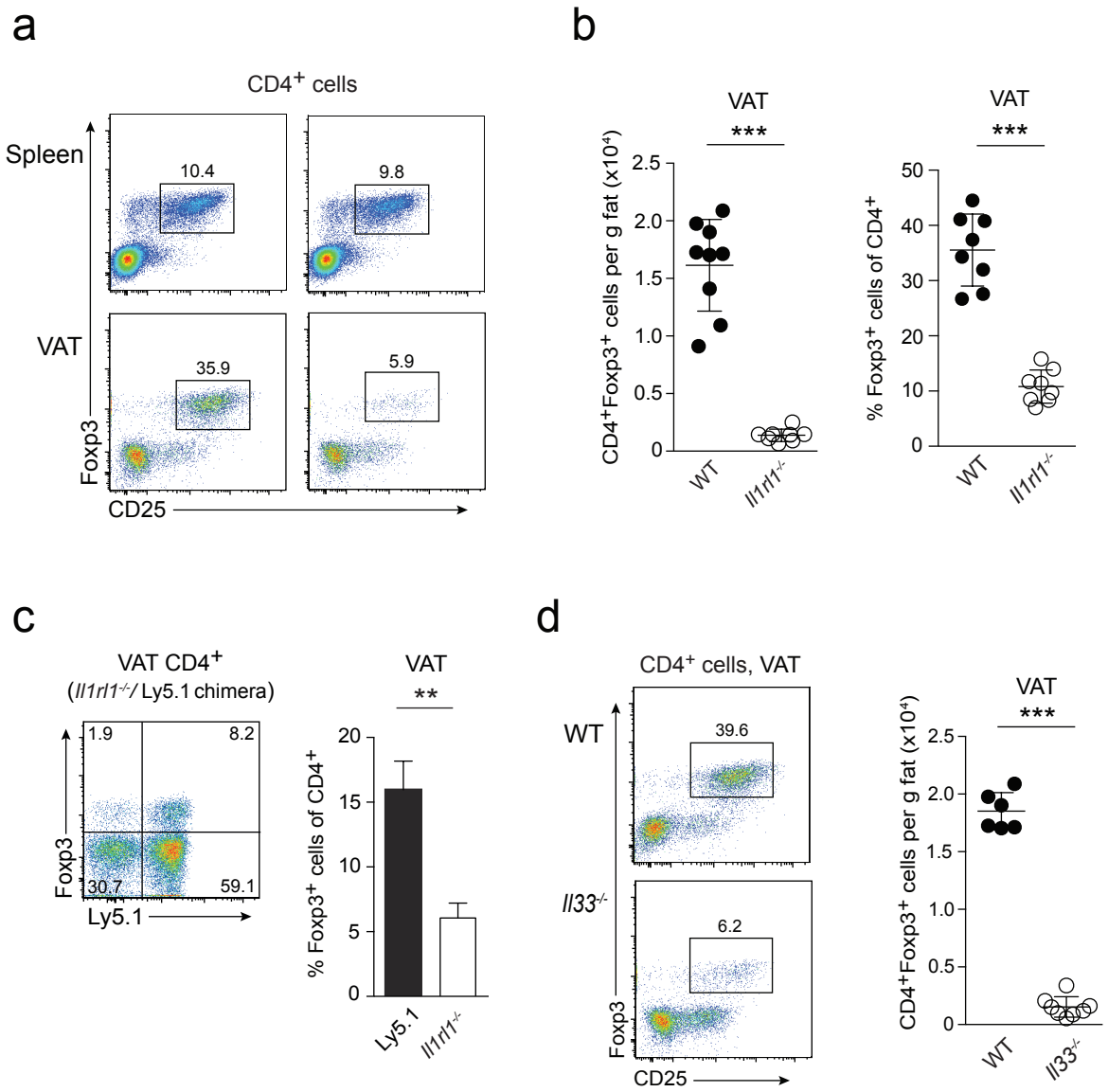

Vasanthakumar et al. Fig. 3

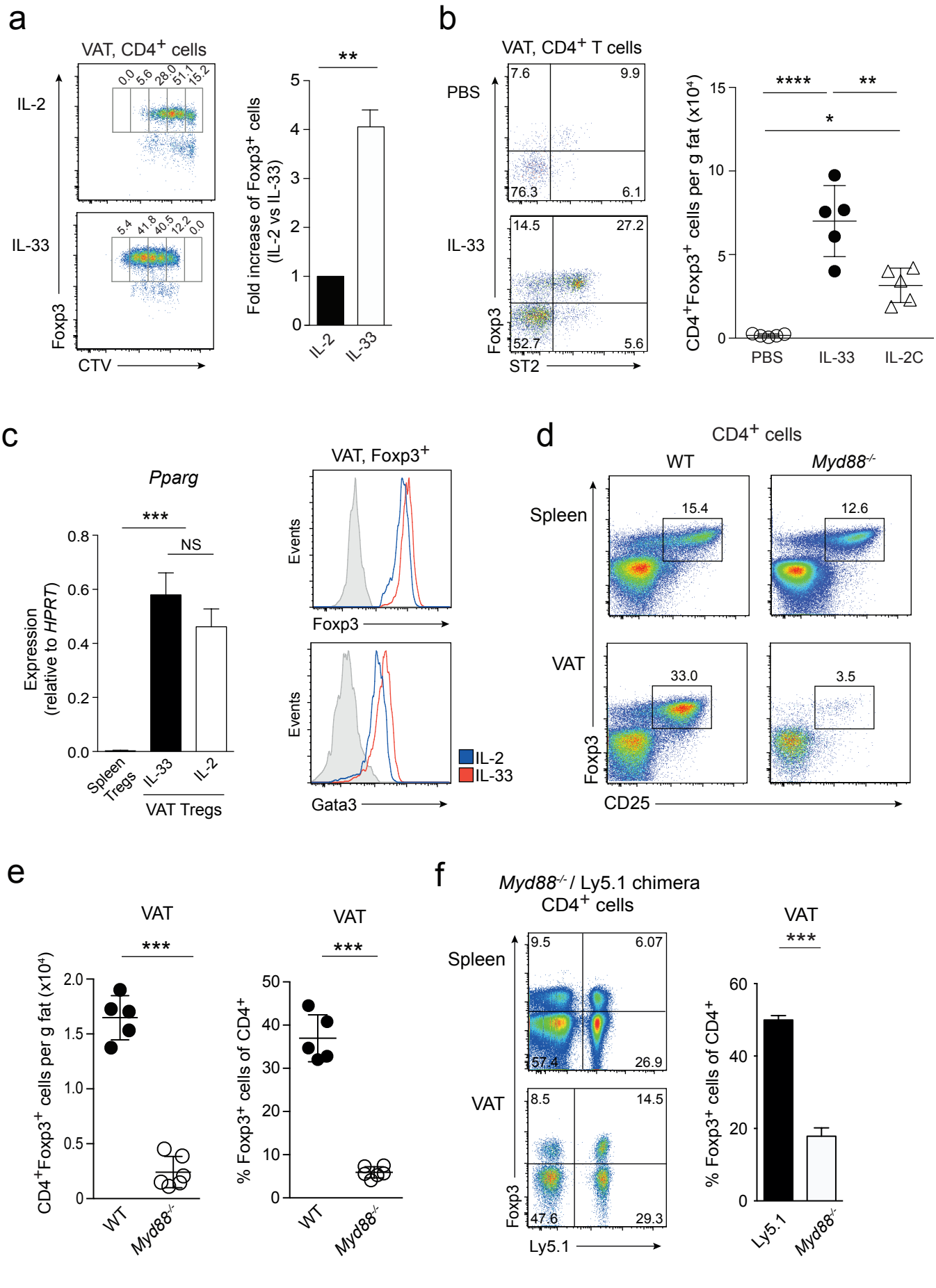

Vasanthakumar et al. Fig. 4

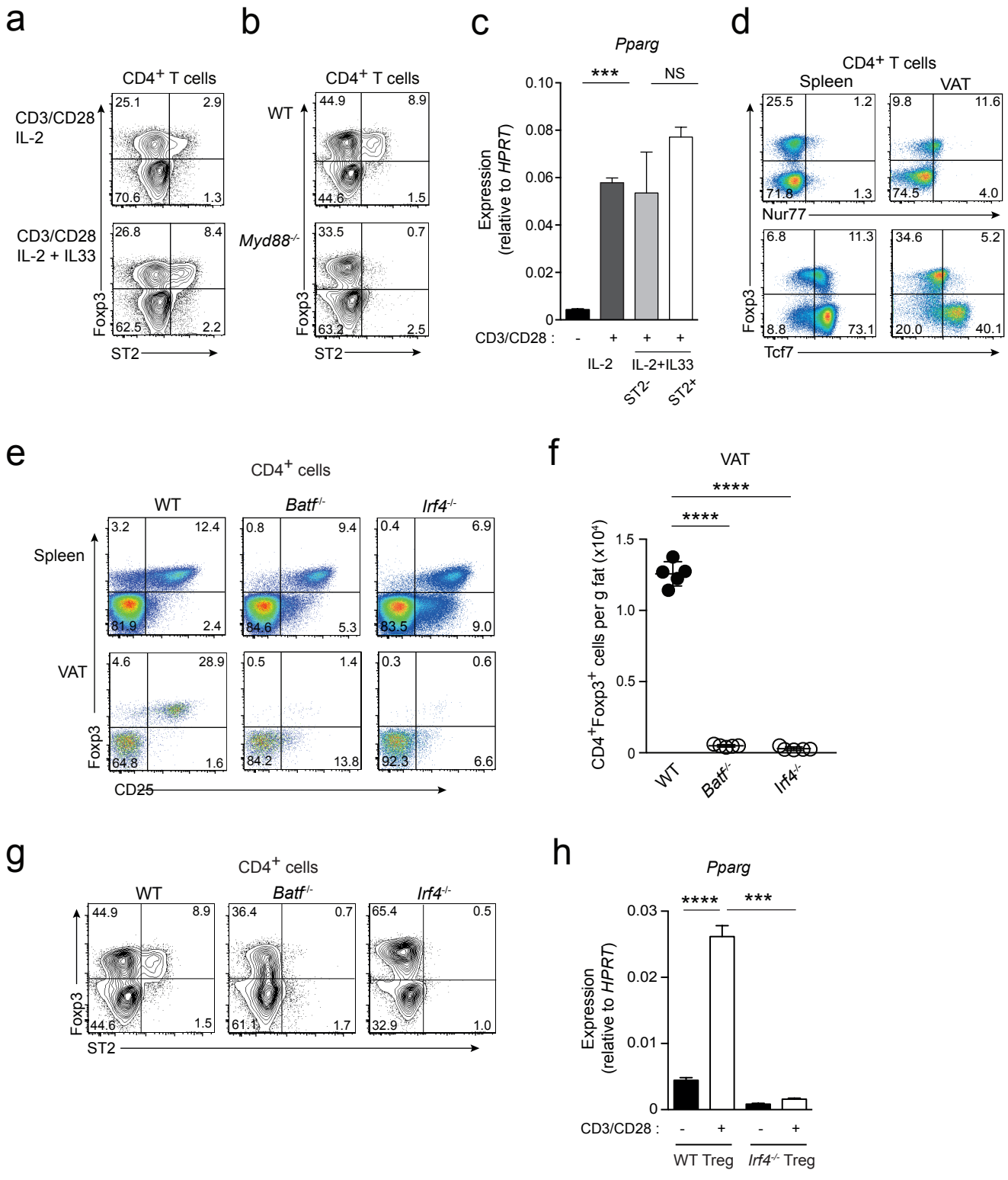

Vasanthakumar et al. Fig. 5

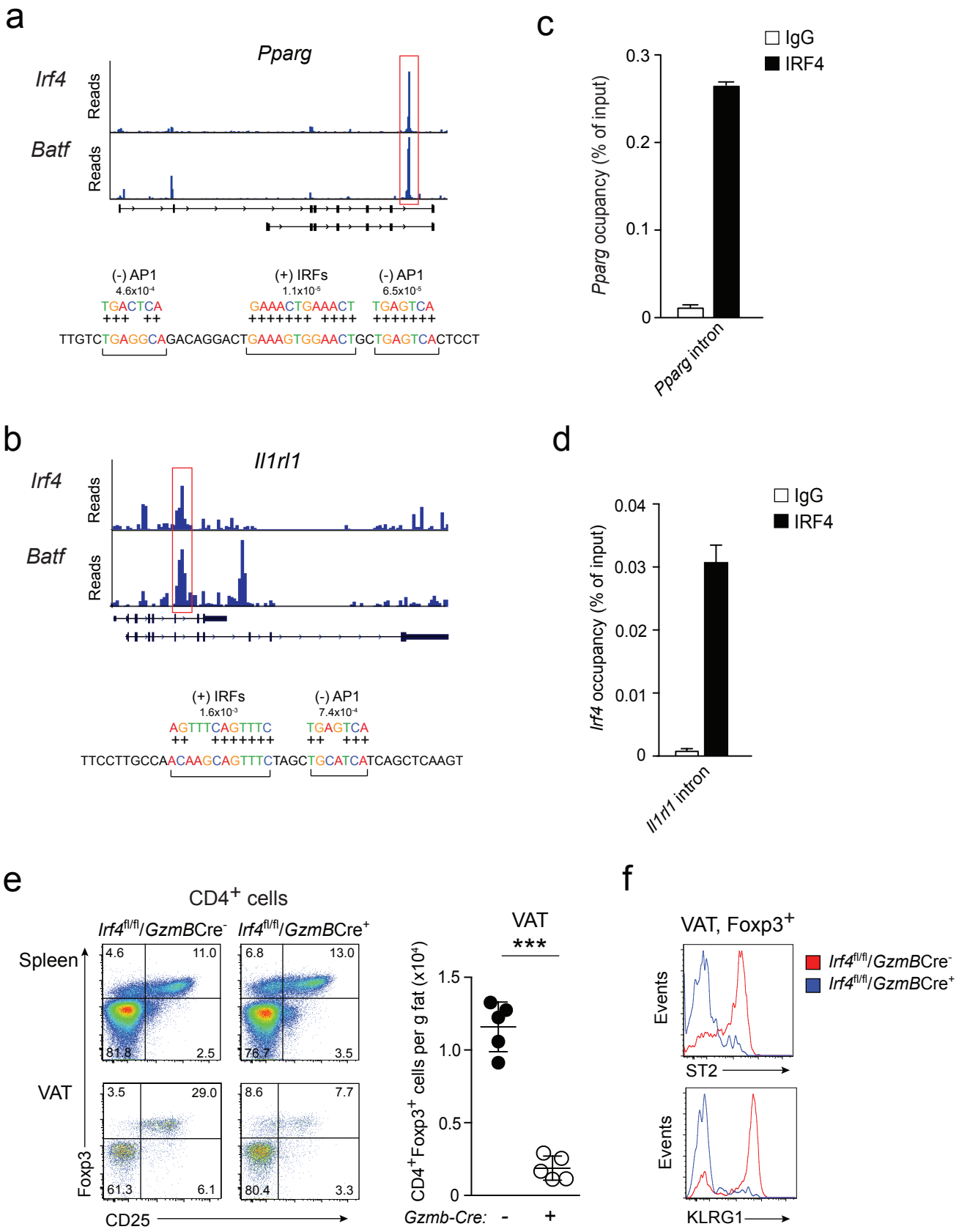

Vasanthakumar et al. Fig. 6

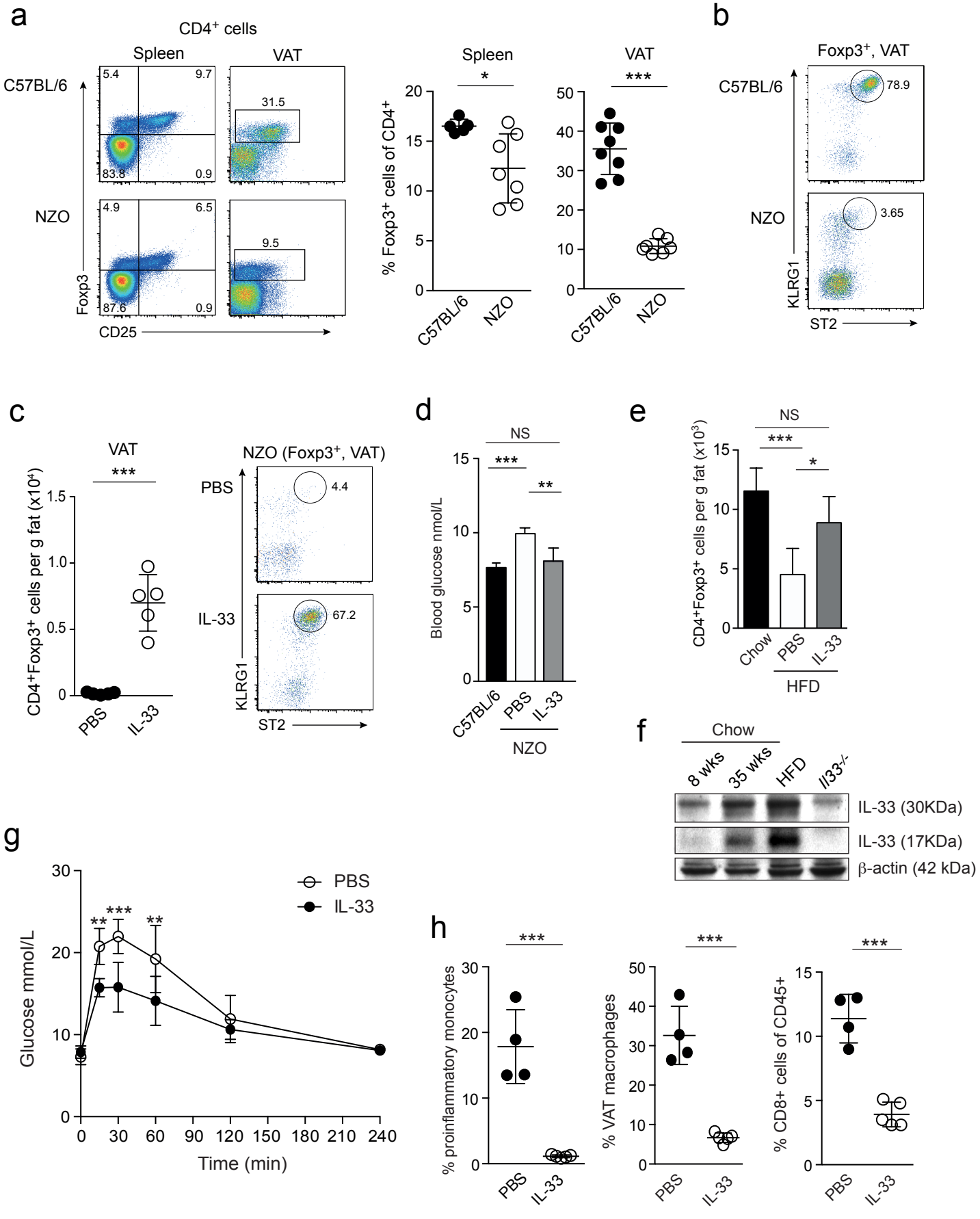

Vasanthakumar et al. Fig. 7

Supplementary Figure Legends

Suppl. Fig. 1. eTregs are a transcriptionally distinct Treg population. (**a**) Gating strategy used to purify Blimp1^{-} cTregs (red gate) and Blimp1^{+} eTregs (green gate) from pooled spleens and lymph nodes (LNs) of *Blimp1*$^{+/GFP}$ mice. Representative of 6 experiments. (**b**) Heat map showing top 100 differentially expressed genes between cTregs and eTregs determined using likelihood ratio test. (**c**) RNAseq tracks showing the expression of *Foxp3* in cTregs and eTregs.

Suppl. Fig. 2. ST2 expression correlates with other VAT-Treg markers. (a) Expression of ST2 and other surface molecules on Treg populations in spleen and VAT as indicated. Flow cytometric plots displaying CD4^{+}Foxp3^{+} cells from a 35-week-old mouse, representative of at least three experiments.

Suppl. Fig. 3. IL-33 is specifically required for VAT-Tregs but dispensable for other Treg populations. (**a-c**) Treg proportions and phenotype in selected lymphoid (a-b) and non-lymphoid (c) organs of wild-type (WT) and *Il1rl1*$^{-/-}$ mice as indicated. Values the means of 3-8 mice per group. LPL - Lamina propria lymphocytes of the small intestine. **(d)** Treg proportions and phenotype in spleens of WT and *Il33*$^{-/-}$ mice as indicated. Values the means of 5 mice per group. **(e)** Weight of VAT from 35-week old *Il1rl1*$^{-/-}$, *Il33*$^{-/-}$ and WT mice. Values are mean from 8 mice per group. (**f-g)** Glucose tolerance tests for *Il1rl1*$^{-/-}$ (f), *Il33*$^{-/-}$ (g) and corresponding control mice. The graphs are representative of at least two independent experiments. Values are means of 3-5 mice per group. Two way ANOVA test ($P<0.0001$), error bars denote S.E.M. **(h)** HOMA-IR calculated for *Il33*$^{-/-}$ and WT mice. **(i)** Results of flow cytometric analysis of *Il33*$^{-/-}$ and WT mice. Graphs show VAT macrophages (TCRβ-, CD11b+, F4/80+ and CD11c+), pro-inflammatory monocytes (TCRβ-, CD11b+ Ly6C+) and CD8 T cells. **(j)** Serum leptin levels in *Il33*$^{-/-}$ mice. Values are mean ± S.D. ** $P<0.008$; * $P<0.04$.

Suppl. Fig. 4. IL-33 drives proliferation of VAT-Tregs. (**a-b**) *In vitro* proliferation of VAT-Tregs. Equal numbers of purified VAT lymphocytes from WT mice were CTV labeled and cultured for 3.5 days with (a) or without (b) plate bound anti-CD3,

soluble anti-CD28, cytokines, and with or without IL-2 blocking antibodies as indicated. Bar graph shows relative numbers of Tregs at the end of the culture. Figure representative of three experiments performed. (**c**) Relative *Il33* transcripts levels in the VAT of young (8 weeks) versus old (35 weeks) mice. (**d**) IL-33 protein expression analyzed by Western Blot of adipose tissue from young versus old mice as indicated on a normal Chow diet. *Il33*$^{-/-}$ mice were used as specificity control. Loading was controlled by detection of an unspecific band with the anti-IL-33 antibody. (**e-f**) ST2 expression on VAT-Tregs isolated from wild-type mice of different ages as indicated (e) and correlation of age and VAT-Treg prevalence. Numbers are mean ± S.D. of at least 5 mice per age group. One way ANOVA for both panels, $P<0.0001$. (**g**) Frequency of Foxp3^{+} cells of CD4^{+} T cells in selected lymphoid and non-lymphoid organs from PBS, IL-33 and IL-2/anti-IL-2 Ab complex (IL-2c) treated mice. Values are the mean ± S.D. from 5 mice per group. LPL - Lamina propria lymphocytes of the small intestine. (**h**) ST2 expression on KLRG1^{+} and KLRG1^{-} Tregs. (**i**) Flow cytometric analysis of splenic Foxp3^{+} cells showing expression of KLRG1 and ST2 in PBS (control) and IL-33 treated mice (left). Graph showing proportion of KLRG1^{+} cells ± S.D. of total Tregs in the spleen in control and IL-33 treated mice (right). (**j**) Proportion of Foxp3^{+} cells within CD4^{+} T cells in the VAT at different time points post IL-33 injection. One way ANOVA, $P=0.0047$. Symbols indicate data points for individual mice, values are mean ± S.D. * $P=0.06$; ** $P<0.008$; *** $P<0.001$.

Suppl. Fig. 5. IL-33 signaling through Myd88 is required for VAT-Treg differentiation. (**a-b**) Proportion of Tregs of CD4^{+} T cells in selected lymphoid (a) and non-lymphoid **(b)** organs of wild-type (WT) and *Myd88*$^{-/-}$ mice. LPL - lamina propria lymphocytes of the small intestine. (**c**) Flow cytometric analysis of Tregs from the lymph nodes (LN) of wild-type and *Myd88*$^{-/-}$ mice assessed for eTreg markers ICOS and KLRG1 (left), frequency of KLRG1^{+} cells of lymph node Tregs from WT and *Myd88*$^{-/-}$ mice (right). Values are mean ± S.D. from 5 mice per group. **(d)** VAT weight from WT and *Myd88*$^{-/-}$ mice. (**e**) Tregs enriched from spleens of wild-type (WT) mice and cultured in the presence of plate bound anti-CD3 antibodies and soluble anti-CD28 and cytokines as indicated for 3 days. Expression of ST2 and Foxp3 is shown. **(f)** Tregs enriched from spleens of WT and *Myd88*$^{-/-}$ mice and cultured in the presence of plate bound anti-CD3 antibodies and soluble anti-CD28,

IL-2 and IL-33 for 3 days. Expression of ST2 (dot plots, left) and proliferation measured by CTV dilution. * P=0.003.

Suppl. Fig. 6. BATF and IRF4 are required for VAT-Treg development. (**a-b**) Proportions of Tregs of $CD4^+$ T cells in the spleens and VAT of wild-type mice in comparison to *Batf*$^{-/-}$ (b) and *Irf4*$^{-/-}$ (b) mice. Values are mean ± S.D. from 5-7 mice per group. **(c-d)** Weight of VAT (c) and body weight (d) of WT, *Irf4*$^{-/-}$ and *Batf*$^{-/-}$ mice. Values are the means from each 6-8 mice per group (one way ANOVA). **(e)** Bar graph showing proportions of WT and knock-out $Foxp3^+$ cells as indicated from the spleens and VAT of Ly5.1 (WT) / *Batf*$^{-/-}$ (left) and Ly5.1 (WT) / *Irf4*$^{-/-}$ peripheral chimeric mice. **(f)** Flow cytometric analysis of ST2 expression on Tregs from the VAT of mice of the indicated genotype. (**g-h**) MACS enriched $CD4^+CD25^+$ cells from WT (Ly5.1), *Batf*$^{-/-}$ (Ly5.2) and *Irf4*$^{-/-}$ (Ly5.2) mice as indicated were mixed as indicated, CTV labeled and cultured in conditions that induce ST2. Flow cytometric analysis of total $Foxp3^+$ cells. Bar graphs show the proportion of $Foxp3^+$ cells of the indicated genotype that express ST2. Histograms (gated on $Foxp3^+$ cells) show CTV dilution profiles. Values are mean ± S.D. from 5 male 30-week-old mice per group. **(i)** RNAseq track showing expression of *GzmB* by cTregs and eTregs. **(j)** Weight of VAT from *Irf4*$^{fl/fl}$ *GzmB-Cre*$^+$ and *GzmB-Cre*$^-$ mice. Values are mean from 4 mice per group. * P<0.03; ** P<0.006; *** P<0.0003; **** P<0.0001

Suppl. Fig. 7. IL-33 administration can rescue VAT-Treg defects in genetically obese and HFD mice. (a) Percentages of VAT Foxp3+ cells within the CD4 compartment from C57BL/6 and NZO mice **(b)** Intraperitoneal glucose tolerance test (GTT) for NZO mice treated with PBS and IL-33. **(c)** Area under curve (AUC) for GTT performed on HFD and NZO mice as indicated. Values are mean from 4 and 5 mice per group. **(d)** Proportion of CD8+ T cells and VAT macrophages in the VAT of NZO mice treated with PBS or IL-33 as indicated. **(e)** Representative flow cytometric analysis of HFD mice. Plots show VAT macrophages (TCRβ-, CD11b+, F4/80+ and CD11c+) and pro-inflammatory monocytes (TCRβ-, CD11b+ Ly6C+). **(f)** Expression of Mcp1, Mip1α, RANTES and IL1β in the VAT of HFD and NZO mice treated with PBS or IL-33 analyzed by qPCR. Values are means ± S.D. For the GTT experiments

in (b) a two way ANOVA test was performed ($P<0.0001$) and error bars denote S.E.M. P values for other graphs * $P<0.05$; * $P<0.003$.

Suppl. Fig. 8. IL-33 treatment increases Treg numbers and improves metabolic parameters in NZO and HFD mice. (a) Weight of VAT isolated from NZO and HFD mice treated with PBS or IL-33. **(b)** H&E staining of VAT sections, numbers of adipocytes per field and adipocyte sizes from PBS and IL-33 treated NZO (upper panels) and HFD mice (lower panels) as indicated. Values are means ± S.E.M. **(c)** HOMA-IR calculated from PBS or IL-33 treated NZO and HFD mice as indicated. **(d)** Western blot showing Akt phosphorylation in VAT of PBS and IL-33 treated NZO or HFD mice after intravenous insulin injection. (**e**) Analysis of ST2 expression on human Tregs from peripheral blood mononuclear cells or omental fat as indicated; representative of three samples. * $P<0.02$; *** $P=0.0002$; **** $P<0.0001$.

a

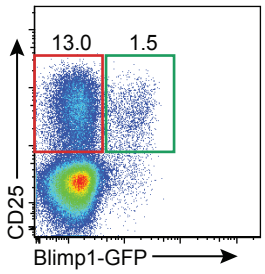

c

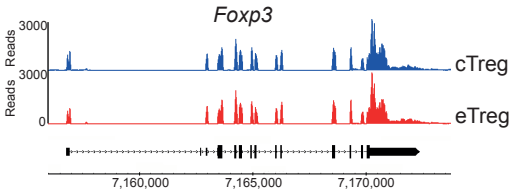

b

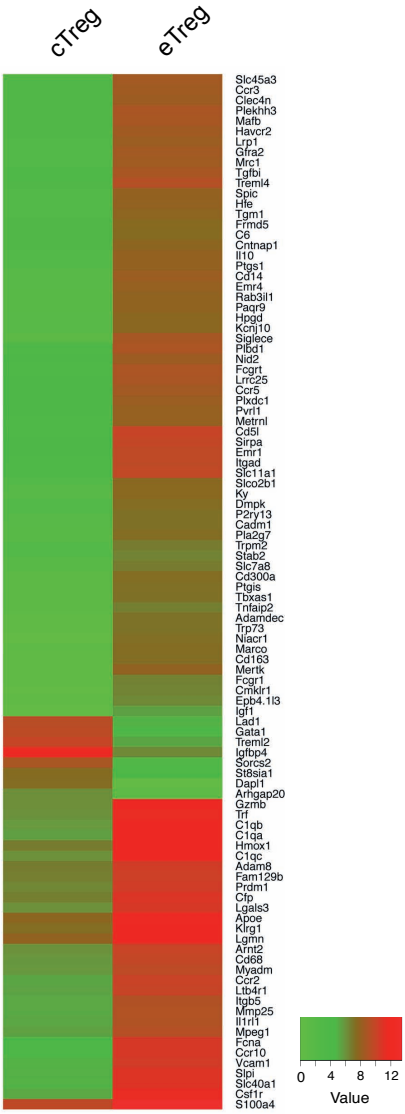

Vasanthakumar et al. Suppl. Fig. 1

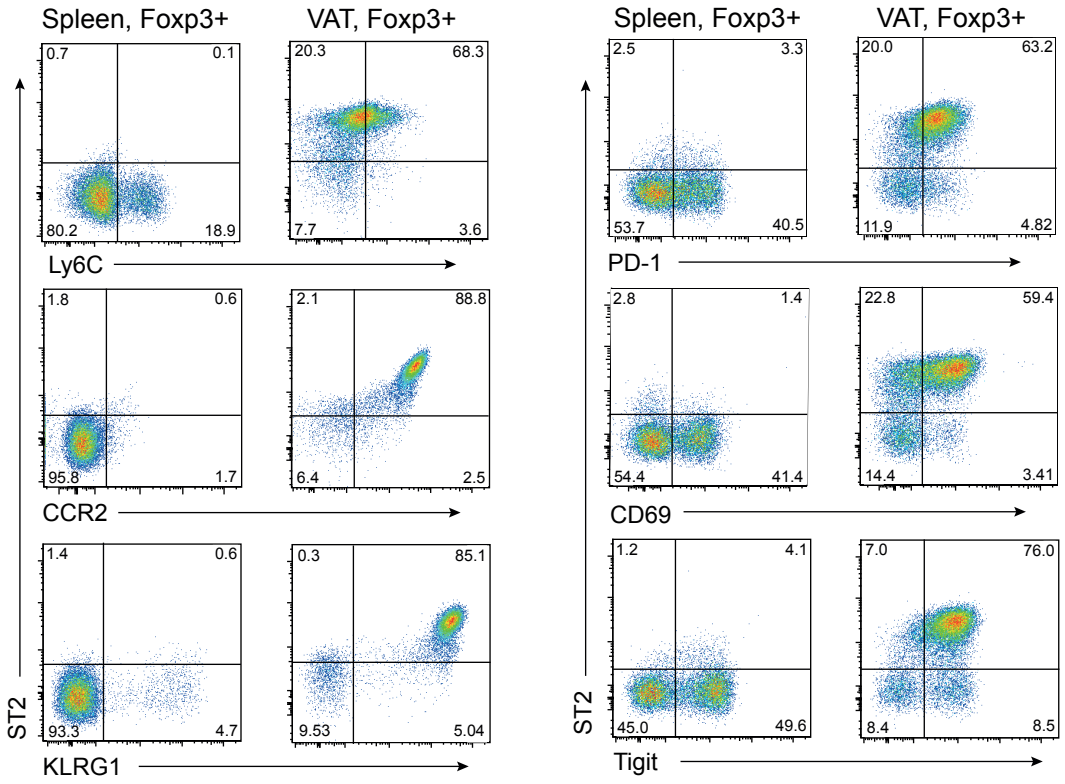

Vasanthakumar et al. Suppl. Fig. 2

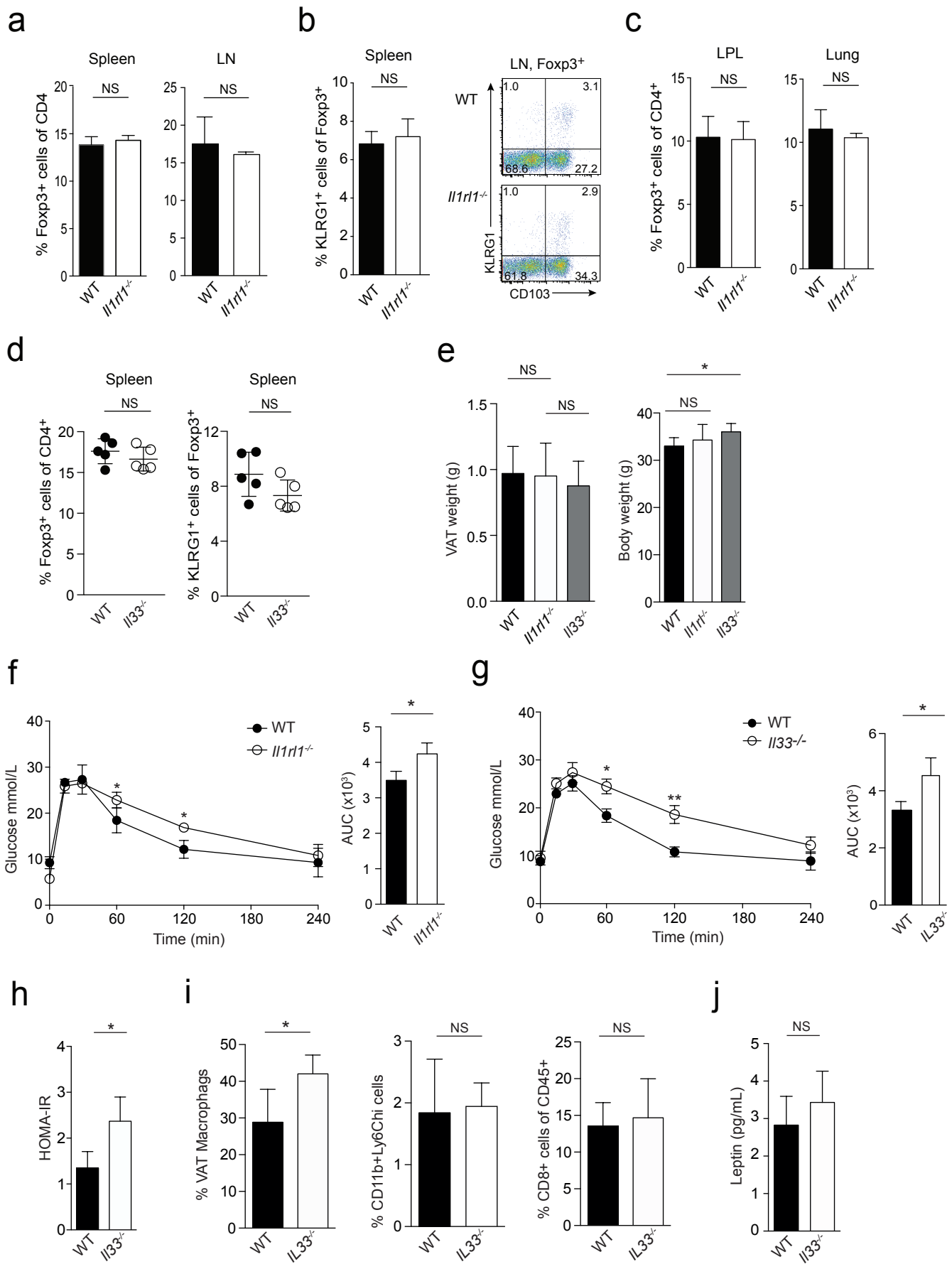

Vasanthakumar et al. Suppl. Fig. 3

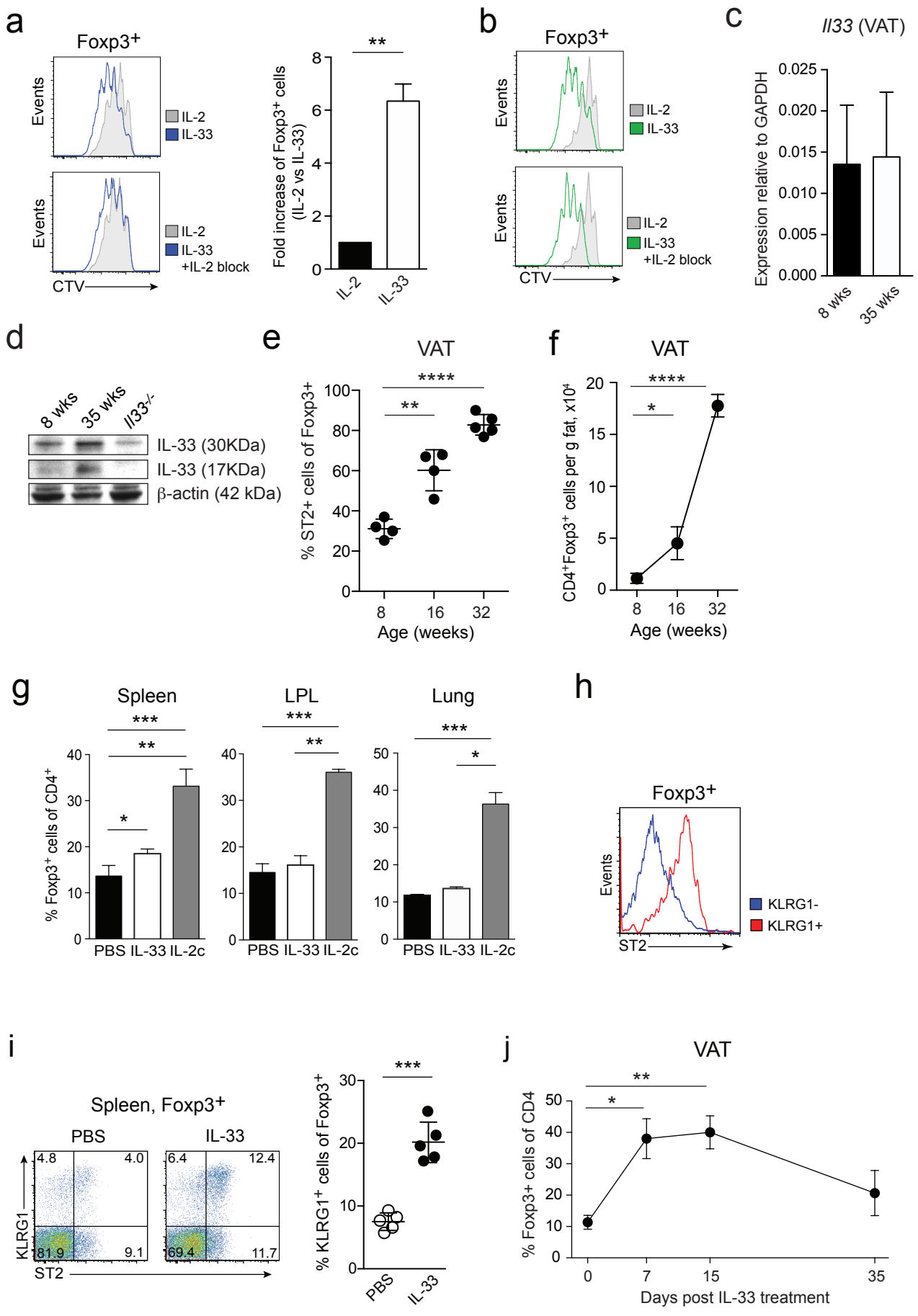

Vasanthakumar et al. Suppl. Fig. 4

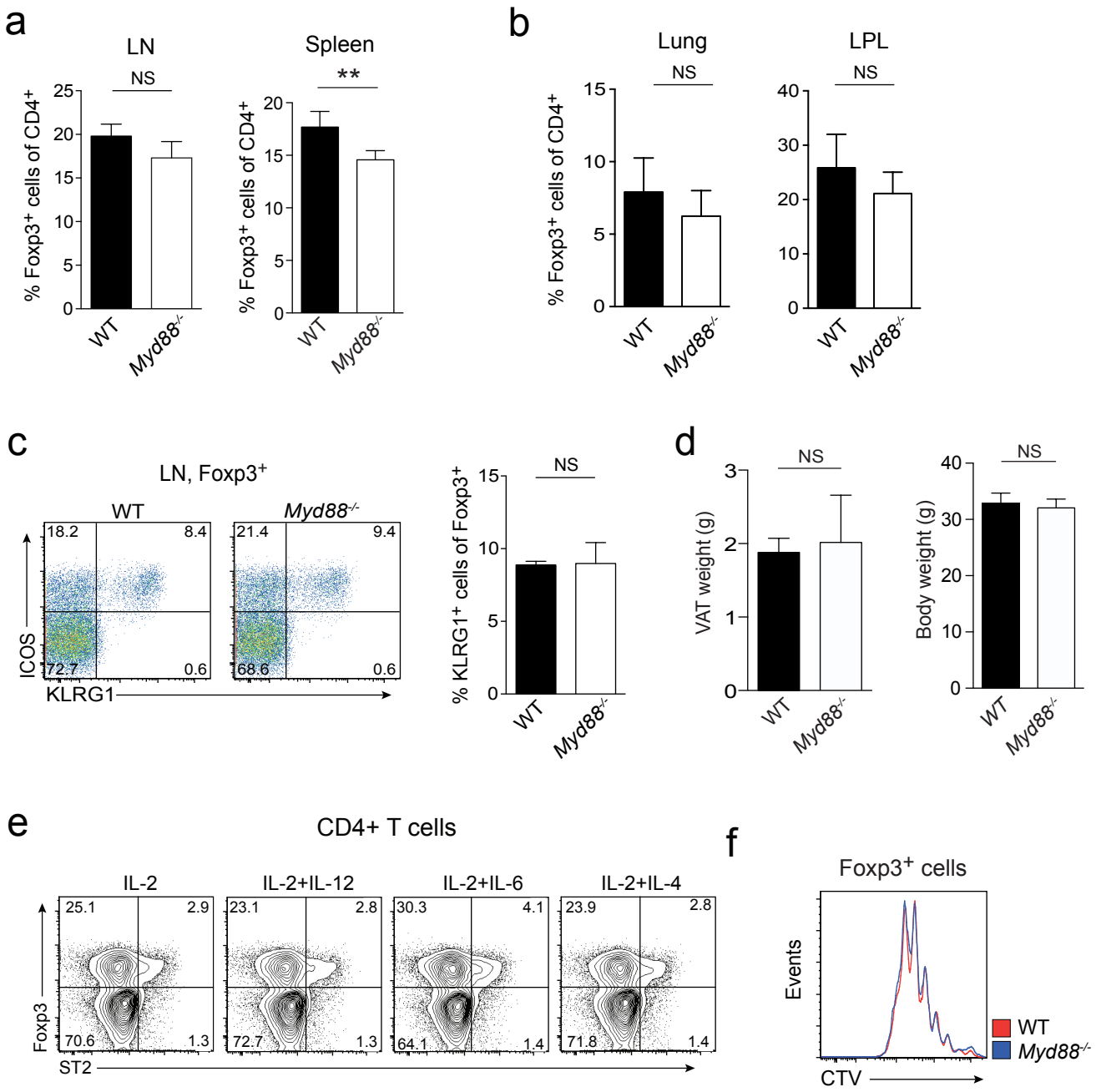

Vasanthakumar et al. Suppl. Fig. 5

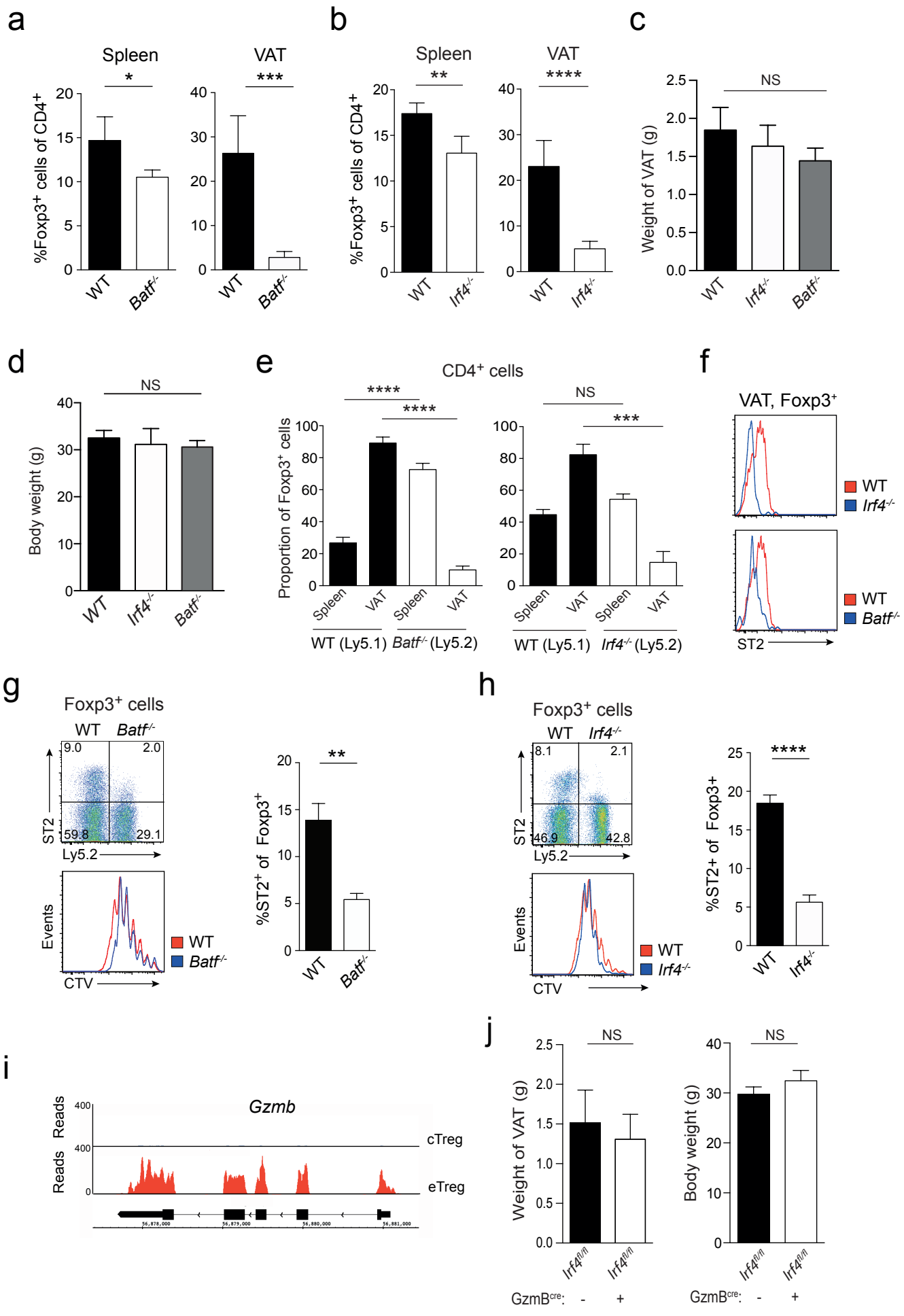

Vasanthakumar et al. Suppl. Fig. 6

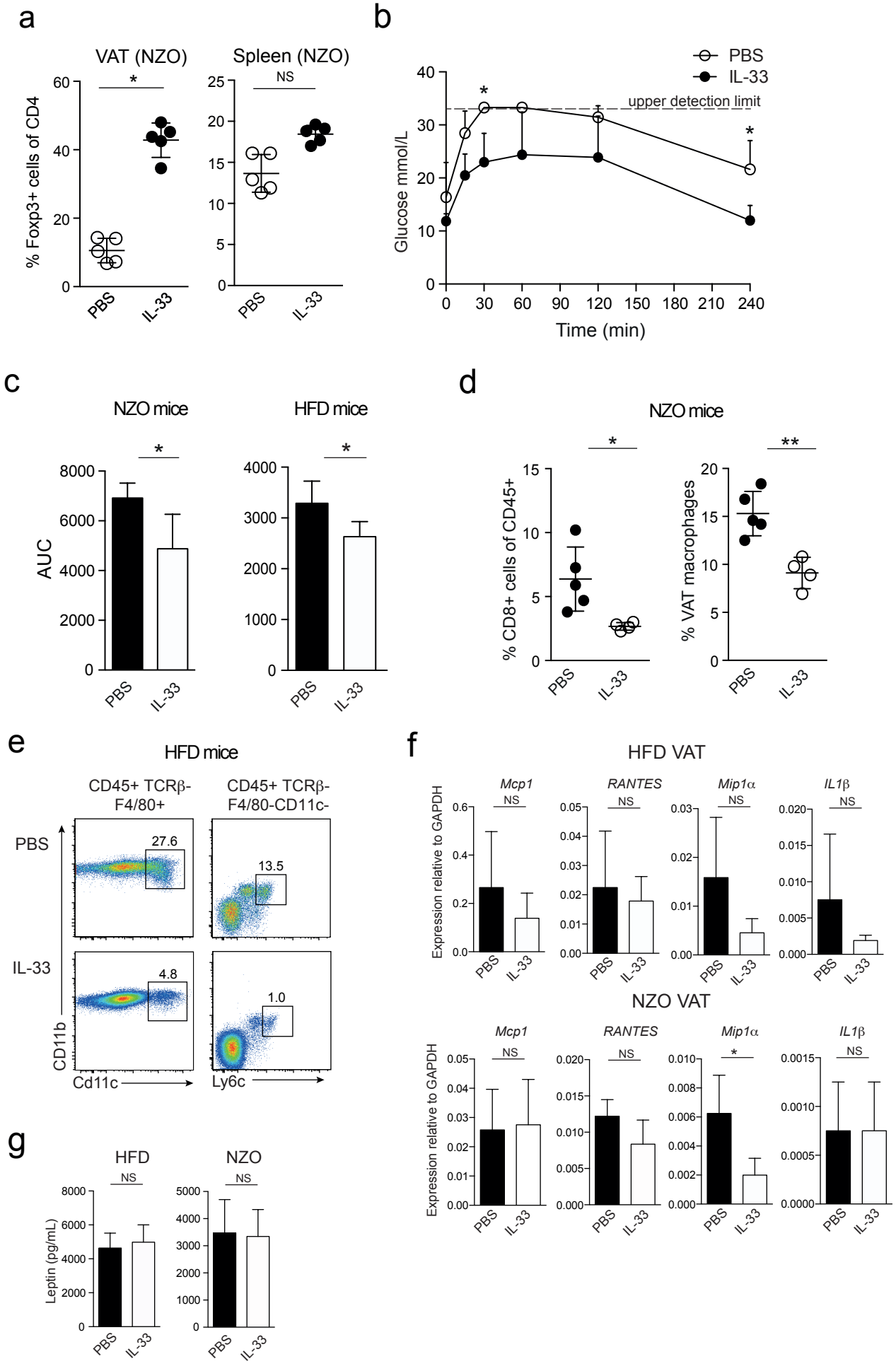

Vasanthakumar et al. Suppl. Fig. 7

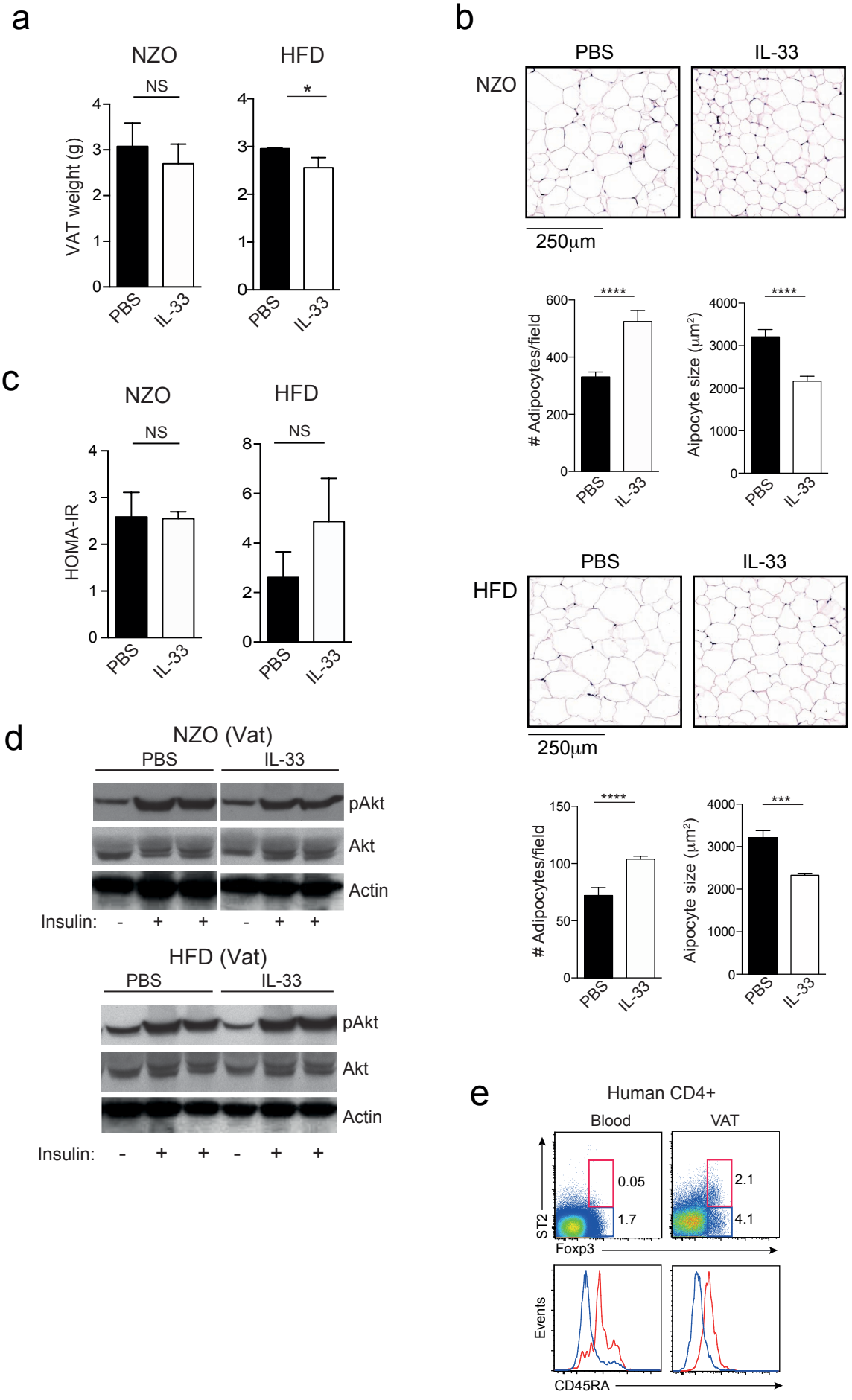

Vasanthakumar et al. Suppl. Fig. 8